ACQUISITION OF A VARDOULAKIS-TYPE PLANE STRAIN DEVICE FOR ADVANCED TESTING OF SOILS

FINAL PROJECT REPORT

by

T. Matthew Evans and Yen Nhi Amy Nguyen
Oregon State University

for
Pacific Northwest Transportation Consortium (PacTrans)
USDOT University Transportation Center for Federal Region 10
University of Washington
More Hall 112, Box 352700
Seattle, WA 98195-2700

In cooperation with US Department of Transportation-Research and Innovative Technology Administration (RITA)

Disclaimer

The contents of this report reflect the views of the authors, who are responsible for the facts and the accuracy of the information presented herein. This document is disseminated under the sponsorship of the U.S. Department of Transportation's University Transportation Centers Program, in the interest of information exchange. The Pacific Northwest Transportation Consortium, the U.S. Government and matching sponsor assume no liability for the contents or use thereof.

Technical Report Documentation Page

1. Report No.	2. Government Accession No.	3. Recipient's Catalog No.
ABC-123-XYZPDQ	8675309	CUL8TRAL1G8R

4. Title and Subtitle	5. Report Date
Acquisition of a Vardoulakis-Type Plane Strain Device for Advanced Testing of Soils	05/31/2018
	6. Performing Organization Code 314159
7. Author(s) T. Matthew Evans and Yen Nhi Amy Nguyen	**8. Performing Organization Report No.** 1
9. Performing Organization Name and Address PacTrans Pacific Northwest Transportation Consortium University Transportation Center for Region 10 University of Washington More Hall 112 Seattle, WA 98195-2700	**10. Work Unit No. (TRAIS)** 37
	11. Contract or Grant No. DTRT13-G-UTC40
12. Sponsoring Organization Name and Address United States of America Department of Transportation Research and Innovative Technology Administration	**13. Type of Report and Period Covered** Final
	14. Sponsoring Agency Code 3597205397

15. Supplementary Notes
Report uploaded at www.pactrans.org

16. Abstract

Plane strain loading conditions are present in many transportation-related geostructures, such as long embankments and behind retaining walls. However, the mechanical properties of soils are not typically characterized in plane strain compression. This is due not to lack of interest but because whereas direct shear and axisymmetric (conventional triaxial) compression equipment is nearly ubiquitous in geotechnical laboratories, plane strain devices are relatively more rare, primarily because of their complexity and expense. This report documents the acquisition, set-up, and trial testing of a Vardoulakis-type plane strain device in the Oregon State University geotechnical laboratory. The device was acquired "used" and "as-is," and significant effort was involved in developing, installing, and testing it. The device is now fully functional. This report serves to document the effort, present sample test results, provide a users' manual, and outline procedures for data collection and reduction.

17. Key Words	18. Distribution Statement
plane strain compression, strain localization, shear banding	No restrictions.

19. Security Classification (of this report)	20. Security Classification (of this page)	21. No. of Pages	22. Price

Form DOT F 1700.7 (8-72) **Reproduction of completed page authorized**

Table of Contents

List of Figures

List of Tables

Acknowledgments

The equipment described in this report was originally owned by Prof. Amy Rechenmacher from the Sonny Astani Department of Civil and Environmental Engineering at the University of Southern California, who graciously provided it to Oregon State University for the cost of shipping. The Oregon State University School of Civil and Construction Engineering was responsible for transporting the device from Los Angeles to beautiful Corvallis, Oregon. It would not have been possible to install the biaxial device in the OSU geotechnical laboratory without the generous support of the Pacific Northwest Transportation Consortium (PacTrans). James Batti was invaluable in setting up the data acquisition system and associated electronics.

We are grateful for all of this support.

Executive Summary

Plane strain loading conditions are present in many transportation-related geostructures, such as long embankments and behind retaining walls. However, the mechanical properties of soils are not typically characterized in plane strain compression. This is due not to lack of interest but because whereas direct shear and axisymmetric (conventional triaxial) compression equipment is nearly ubiquitous in geotechnical laboratories, plane strain devices are relatively more rare, primarily because of their complexity and expense. This report documents the acquisition, set-up, and trial testing of a Vardoulakis-type plane strain device in the Oregon State University geotechnical laboratory. The device was acquired "used" and "as-is," and significant effort was involved in developing, installing, and testing the device. The device is now fully functional. This report serves to document the effort, present sample test results, provide a users' manual, and outline procedures for data collection and reduction.

Chapter 1 Introduction

It is well-known that all three principal stresses play a role in the stress-strain-strengthvolume change response of solids and granular materials. However, conventional axisymmetric compression and direct shear tests can only reproduce relatively simple stress geometries. Nonetheless, these tests are typically used to approximate design strength parameters for soils, even when field conditions may be plane strain (e.g., long embankments, earth dams, retaining structures, landslide slip surfaces).

The drawback of this approach is that in soils, strain localization ("shear banding") consists of shear failure along a well-defined plane of high strain. This plane is of some finite thickness and characterized by high void ratios relative to the surrounding soil. Shear banding is evidenced in many field-scale failures of geotechnical systems, including shallow foundations, slopes, and earth retaining structures. Indeed, the presence of shear bands is implicitly suggested by both the Coulomb and Rankine earth pressure theories, which are the most common bases for strength design of geotechnical structures.

Over the past three decades, there has been increased interest in understanding the mechanics of these shear bands. The problem is of interest to engineers and scientists in a wide range of disciplines: geotechnical engineering, physics, mathematics, structural geology, chemical engineering, and agricultural engineering. Across all of these disciplines, the driving force behind the research is broadly defined as the desire to minimize the adverse effects of localization, whether it be behind a retaining wall or in considering hopper flow (wherein localization can lead to material segregation).

The equipment described herein is uniquely capable of producing kinematically unconstrained shear bands in soils under plane strain load geometry. This report serves to

document the acquisition, installation, and calibration of a used Vardoulakis-type plane strain compression device. The document is organized in the following manner:

- Chapter 2 provides a brief review of existing literature on plane strain testing of soils;
- Chapter 3 describes the device's acquisition and installation;
- Chapter 4 presents the experimental methods;
- Chapter 5 summarizes some experimental results; and
- Chapter 6 presents a summary of the work performed and any conclusions that may be drawn from it.

References and appendices are presented at the end of this report.

Chapter 2 Literature Review

2.1 Overview

The most common laboratory tests for determining the stress-strain-strength response of granular materials are the conventional triaxial compression (CTC) and direct shear (DS) tests. However, each of these tests has drawbacks, particularly with respect to the study of strain localizations. In the CTC test, applied stresses by definition are axisymmetric, providing no control over the intermediate principal stress. The CTC test is designed to induce homogenous deformation for the study of the constitutive behavior of soils, and if shear banding does occur, then localization geometries are typically complex fan-shaped patterns (Desrues et al., 1996; Alshibli et al., 2000) not likely to be encountered *in-situ*. The DS test, by contrast, forces failure via a localized region of high strains, but this region is predetermined by the test device geometry and not allowed to occur along its natural plane within the specimen.

The use of plane strain (PS) and true triaxial (TT) tests is becoming increasingly more widespread for the characterization of the stress-strain-strength response of granular soils, particularly when strain localization is being studied (e.g., Drescher et al., 1990; Lade and Wang, 2001; Evans and Frost 2010). The TT test has the advantage that all three principal stresses are controlled during testing, allowing for the attainment of a wide variety of loading conditions. The PS test is effectively a specific implementation of the more complex TT test, wherein the major and minor principal stresses are controlled and the intermediate principal stress is measured on the plane defined by an axis of zero deformation.

2.2 Plane Strain versus Axisymmetric Compression

The PS (or biaxial) compression test has been used since the 1930s as a tool for evaluating the stress-strain-strength response of soils (Kjellman, 1936). Results from PS and TT compression tests were compared to those obtained with a type of direct shear (DS) device

known as the Krey shearing apparatus. A friction angle of 43◦ was measured for the sand in PS compression, versus 35◦ in TT (axisymmetric) compression and 34◦ in DS. Kjellman (1936) also mentioned that deformation in the DS device was 10 times greater at the end of the test than that in the PS test. This may indicate that the measurement in the Kjellman soil testing device was the peak friction angle, while the DS test was measuring the critical state friction angle.

Perhaps the largest body of work concerning PS compression tests on soils is focused on identifying the role of intermediate principal stress on soil strength or the effects of loading conditions on macroscopic material response (Cornforth, 1964; Henkel and Wade, 1966; Rowe, 1969; Lee, 1970). Cornforth focused on the effects of strain influence on the strength of sand, rooted in the argument that the loading conditions for many geotechnical applications (e.g., retaining walls and embankment dams) are more closely approximated by the plane strain condition than the axisymmetric triaxial case. In comparing results from PS and CTC tests with the same initial void ratio, Cornforth found that the peak friction angle for PS specimens was consistently 0.5° to 4° greater than for CTC specimens and that axial strains at failure were nearly three times greater in CTC specimens than in PS specimens.

Henkel and Wade (1966) used the same PS apparatus as Cornforth to study the effect of the intermediate effective stress on Weald clay. Both PS and CTC tests were performed on K_0-consolidated specimens, and CTC tests were also performed on hydrostatically consolidated specimens. The undrained shear strength of Weald clay was found to be greatest in the hydrostatically consolidated CTC specimens, followed by the K_0-consolidated PS specimens. Significantly, among the K_0-consolidated specimens, pore pressure generation was greater in the PS tests than in the CTC tests.

Rowe (1969) compared the results of PS, CTC, and DS tests on quartz sand, feldspar, crushed glass, and glass ballotini. In all cases, he found that the maximum angle of internal

friction (φ_{max}) was greater in plane strain than in CTC or DS, in spite of the fact that for a given material the angle of friction between particles (φ_{μ}) and the constant volume friction angle (φ_{cv}) are constant. Rowe's work implied that DS and PS friction angles are related through the constant volume friction angle:

$$\tan\left(\phi'_{ds}\right) = \tan\left(\phi'_{ps}\right)\cos\left(\phi'_{cv}\right) \tag{2.1}$$

where φ'_{dddd} and φ'_{ppdd} are friction angles in direct shear and plane strain, respectively, and φ'_{cccc} is the constant volume friction angle. Therefore, the strength measured in DS will always be less than that measured in PS.

Lee (1970) provided an overview of previous work on the comparison of results from PS and CTC tests. In the overview, Lee considered both "typical" PS testing (i.e., tests on right orthorhombic specimens) and torsional/hollow cylinder tests. The overall conclusion from analyzing these previous data indicated that the plane strain friction angle was consistently greater than the triaxial friction angle (by as much as 8°), but there was some scatter in the data. Lee also highlighted the effects of load geometry on elastic parameters, noting that for a linear elastic material:

$$E_p = \frac{E_t}{1 - \nu_t^2} \tag{2.2}$$

$$\nu_p = \frac{\nu_t}{1 - \nu_t} \tag{2.3}$$

where EE_{tt} and EE_{pp} are the elastic moduli for CTC and PS tests, respectively, and $\nu\nu_{tt}$ and $\nu\nu_{pp}$ are the Poisson's ratios for CTC and PS tests, respectively. Note that equations (2.2) and (2.3) were derived from the constitutive relationships for a linear elastic material given known test conditions for both CTC and PS tests. Figures 2.1 and 2.2 illustrate the theoretical relationships between elastic parameters from the CTC and PS tests described by equations (2.2) and (2.3).

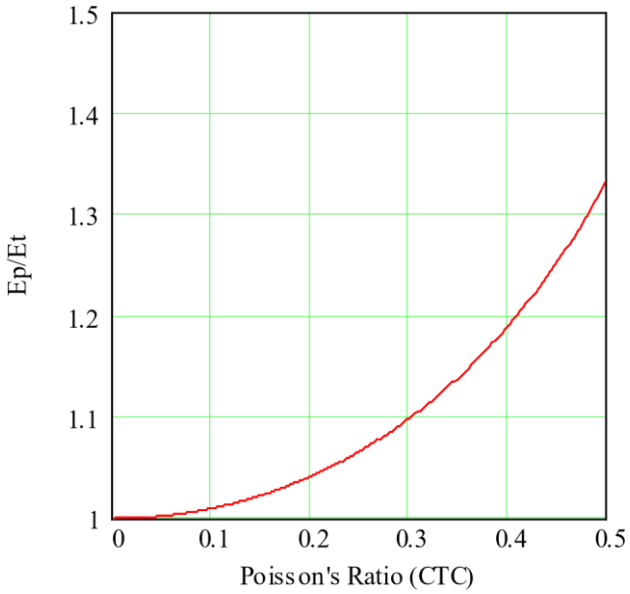

Figure 2.1 Ratio of PS elastic modulus to CTC elastic modulus for a linear elastic material

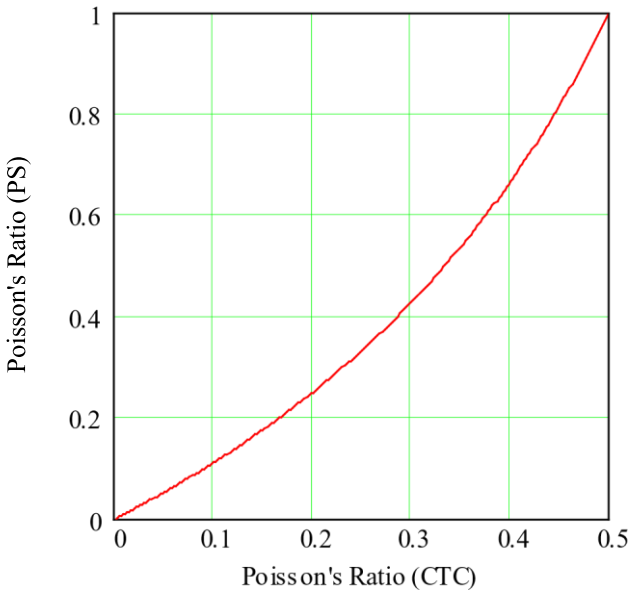

Figure 2.2 Relationship between CTC and PS Poisson's ratios for a linear elastic material

Lee (1970) also performed PS and CTC tests on specimens of Antioch sand and compared the results of tests performed under different loading conditions but with identical starting points in critical state space. Similarly to previous studies, Lee determined that the initial tangent modulus and peak friction angle were greater in the PS tests, while strain to peak was greater in the CTC tests. Additionally, the Poisson's ratios were higher in PS than in CTC and agreed well with linear elastic theor,y as outlined in equation (2.3).

Bolton (1986) analyzed previously published data for 17 different sands in CTC and PS compression to study the effects of dilatancy on sand behavior. This work provided an overview of the effects of dilation on the strength of sand and demonstrated mathematically why a freeforming failure surface is required (through the angle of dilatancy) to be of log spiral form. The dilatancy index was empirically developed as a means of calculating the maximum angle of internal friction and quantifying rates of strain based on observations from laboratory data. The work by Bolton allowed for the incorporation of dilatancy effects into practical design problems,

although Bolton noted that this was often not done in practice, leading to overly conservative designs.

2.3 Strain Localization in Plane Strain Compression

While the work discussed above typically focused on the differences in measurements between PS and CTC testing, an additional body of work (e.g., Vardoulakis, 1980) focused more on the understanding of strain localization (specifically, shear banding) during PS compression and on the calibration of constitutive models to describe shear banding. The two most historically significant theoretical solutions for shear band (i.e., failure plane) inclination were given by Coulomb (1773) and Roscoe (1970) and may be expressed as follows:

$$\theta_C = \frac{\pi}{4} + \frac{\phi_p}{2} \tag{2.4}$$

$$\theta_R = \frac{\pi}{4} + \frac{\Psi_p}{2} \tag{2.5}$$

where $\theta\theta_{CC}$ and $\theta\theta_{RR}$ are the shear band inclinations predicted by Coulomb and Roscoe, respectively; φ'_{pp} is the peak friction angle; and $\psi\psi_{pp}$ is the angle of dilatancy at peak. In the work by Vardoulakis (1980), shear band formation in PS tests on dry sand was considered as a bifurcation problem, yielding the Roscoe and Coulomb angles as the two real solutions for the inclination of the shear band.

Vardoulakis (1980) concluded that theoretically, because there is a lack of normality (i.e., the incremental plastic strain tensor is not orthogonal to the yield locus) during localization of sands subjected to PS loading, localization must always occur in the strain hardening regime (see Nova (2004) for a thermodynamic explanation of why the associated flow rule does not apply to

the localization of purely frictional materials) and that the Coulomb angle of inclination from equation (2.4) above is possible only at peak. The Roscoe solution from equation (2.5) above was shown to be the lower bound for the inclination of the shear band. Using trigonometric approximations and assuming that localization occurs near peak, an approximate solution to the bifurcation problem is the same as the solution first proposed by Arthur, et al. (1977):

$$\theta_A = \frac{\pi}{4} + \frac{1}{4}\left(\phi_p + \psi_p\right) \tag{2.6}$$

where $\theta\theta_{AA}$ is the Arthur prediction for shear band inclination.

For comparison with theory, Vardoulakis (1980) presented results from a series of 20 PS tests on Karlsruhe sand prepared at varying initial void ratios. The measured shear band inclinations from those tests fell approximately halfway between those calculated from the Coulomb or Roscoe theory but agreed very well with both the exact and approximate bifurcation solutions.

2.4 The Vardoulakis-Type Plane Strain Device

The design of a "biaxial device" for PS testing of soils was largely described in the work of Drescher et al. (1990). The design of this biaxial device was significant in that the bottom platen on which the soil specimen rests is affixed to a frictionless linear sled that translates in a direction parallel to the normal of the plane defined by the minor principal stress during testing. Therefore, once the shear band is fully formed, the two theoretical rigid blocks defined by the specimen boundaries and the shear band translate freely with respect to one another. This ensures that post failure deformation is due solely to rigid block displacement, allowing for the constitutive study of soil behavior both before and after the onset of localization.

Drescher, et al. (1990) performed a series of PS tests on specimens of ASTM C190 quartz sand to demonstrate the use of the biaxial device and the proper data reduction and evaluation procedures. The test results showed that the onset of localization was clearly indicated by monitoring sled displacement (i.e., there is very little sled movement prior to localization). They noted two difficulties associated with the biaxial compression test: (i) there was some small amount of sled movement at the very beginning of the test, prior to the onset of localization; and (ii) the shear band tended to daylight very near the upper loading platen. Both difficulties could most likely be attributed to a slight misalignment of the specimen within the device. The authors found that the small amount of sled movement at the beginning of the test corresponded to a self-alignment of the specimen to some equilibrium configuration and was not preventable. However, stress concentrations might still be present at the upper corners of the specimen, leading to the daylight of the shear band near the top platen. To overcome this problem, they constructed inhomogeneous specimens with a zone of loose sand near the center of the specimen. This forced the localization to occur closer to the center of the specimen and did not appreciably affect macroscopic response.

Using the same device outlined by Drescher, et al. (1990), Han and Vardoulakis (1991) investigated the behavior of water-saturated, fine-grained sand subjected to plane strain compression. Specimens of St. Peter Sandstone sand were prepared using moist tamping and tested under drained and undrained conditions. They noted that shear banding occurred in the undrained tests only when the induced pore water pressures were negative (indicating that the specimen was dilatant) and that shear bands formed during strain softening. In drained tests, however, shear bands formed during strain hardening, which is consistent with bifurcation theory (Vardoulakis, 1980). The data from these tests were further analyzed in later work (Vardoulakis, 1996a, 1996b) to assess the applicability of elastoplastic continuum theory for describing the

undrained and drained behavior of sands in plane strain compression using effective stress principles (Terzaghi, 1936). Vardoulakis concluded that for undrained tests a continuum approach was sufficient but that for drained tests the problem was mathematically ill-posed if the soil grains and water were allowed to move with different velocities.

The same biaxial device was next used by Han and Drescher (1993) to study the behavior of poorly graded dry sand under PS compression. Tests were performed on Ottawa sand (ASTM C-190, $dd_{50} = 0.72\ mmmm$) at various confining stresses ($\sigma\sigma'_{cc} = 50, 100, 200, 400\ kkkkkk$). They found that shear band inclination was less than the Coulomb prediction (eq. 2.4) for all confining stresses and that it approached the Roscoe prediction (eq. 2.5) from above at higher confining stresses. This is consistent with theoretical results (Vermeer, 1990) which indicated that for coarse sands, shear bands with stress discontinuities were unlikely to develop, and thus Roscoe-type shear bands should form. Vermeer's analysis followed from the fact that the membrane will not be able to support large out-of-balance forces at the ends of the shear band and was based on the assumption that the shear band thickness is proportional to the mean particle size of the soil (i.e., a larger particle size will generate a larger out-of-balance force).

Because soils are often treated as continua, shear bands in plane strain compression are often studied and described using continuum constitutive models of varying complexity. In these studies, shear bands are modeled using energy considerations and an empirically derived internal length scale. There has also been work on the effects of particle characteristics on shear bands (Yoshida et al., 1994; Yoshida and Tatsuoka, 1997; Alshibli and Sture, 2000; Cho, 2001; Dodds, 2003). The role of the mean particle diameter (dd_{50}) in shear banding is considered to be well understood and is largely considered to affect shear band thickness. Yoshida and Tatsuoka (1997) found that particle shape have little influence on shear band deformation in plane strain

compression tests, but Dodds (2003) noted that angular particles are less likely to form strain localizations because of rotational frustration. On the basis of plane strain tests of fine (subrounded), medium (subangular), and coarse (angular) sands, Alshibli and Sture (2000) found that increasing particle angularity resulted in greater axial strain prior to localization and a less dramatic softening after localization. They noted also that increasing particle angularity resulted in a decrease in the shear band inclination at low (15 kPa) and high (100 kPa) confining stresses. Note, however, that in this study both particle size and shape were changing simultaneously and, therefore, it was difficult to separate the effects of one parameter from the other.

Chapter 3 Device Acquisition and Development

3.1 Overview

The biaxial device described herein was acquired from the geotechnical laboratory at the University of Southern California (USC). Thuserefore, it was used and heavily modified from its manufactured state. The original device included no information with regard to operation, assembly, power supply, or data acquisition. The modifications performed at USC were well documented but were based on the implicit assumption that the device would be used, undisturbed, in that laboratory. Setting the device up after relocating it to a different laboratory with different boundary conditions proved to be a significant challenge, owing to the complexity of the system. Therefore, much of the work described herein was devoted to assembling, modifying, and installing the biaxial device in the OSU laboratory.

3.2 Device Development

Once the biaxial device had arrived at OSU, an inventory was performed to assess the existing components and the items necessary to make it operational in the OSU geotechnical lab. The necessary equipment was split into two categories: base test equipment and data acquisition. Little replacement equipment was needed for the base test. However, putting together a data acquisition system for the OSU lab comprised most of the work.

Load cells and displacement transducers require a data acquisition system. Systems either measure voltage outputs or condition signals to read load and displacement directly. The device received had previously used the latter type. The system consists of a National Instruments (NI) terminal block (SCXI-1315), an LVDT module (SCXI-1540), and two strain/bridge modules (SCXI-1520). The modules measure the readings from the load cell and displacement transducers. The module is then connected to the terminal block. The terminal block conditions

and sends the readings to an NI LabVIEW program. As received, the automated data recording and axial loading commands were programmed into a custom LabVIEW file. While this was an appropriate failsafe mechanism, it proved to significantly complicate device setup (e.g., testing individual device components within the LabVIEW environment). The load cells, displacement transducers, and axial loader could most easily and economically be reused if the same data acquisition system was used. The OSU geotechnical laboratory already owned a strain/bridge module (SCXI-1520); to effectively use this, an NI terminal block (SCXI-1315), and a module (SCXI-1540) were purchased. Once the new system had been connected, the automated data recording LabVIEW program was tested. Load cell and LVDT operation was tested by applying deformations and observing electrical excitation. All sensors were observed to be behaving appropriately. Sensors were not specifically calibrated.

The biaxial device uses a non-polar and chemically inert confining fluid. This is because the load cells and LVDTs are in contact with the specimen and submersed in the fluid. Fluids used previously had been compressed air and low viscosity silicone oil. Both fluids can be difficult to use in testing. Compressed air requires careful set up to prevent high pressure gradients from damaging equipment and is potentially unsafe because of the volume of air required to achieve the desired confining pressures. Silicone oil is expensive and difficult to remove from surfaces. After both options had been evaluated, silicone oil was selected for safety reasons.

3.3 Initial Testing

Because of the difficulties associated with applying external confinement, as described above, preliminary tests were performed without a confining fluid. Specimens were instead vacuum consolidated. The purpose of the preliminary tests was to troubleshoot the data

acquisition system and the LabVIEW program. Initial test results were erroneous because setting up the correct wiring diagram was a trial and error process. However, granular soils tested in this device will always fail via shear banding (Drescher et al. 1990), so qualitative observations were possible. Therefore, while there were no data to process, a visible shear band formed during these tests, as seen in figure 3.1. Once a working wiring diagram had been developed and shear bands consistently formed during testing, additional tests were performed under vacuum. The results from two vacuum-consolidated tests are presented in Chapter 5.

Figure 3.1 Shear band from a preliminary test with no recorded data

Using vacuum to confine specimens works only on dry specimens. If drained and undrained tests on saturated specimens are desired, then external confinement is required. The specimen may be filled with water and back pressured, while the oil is used to apply a uniform confining pressure on all three planes. Initial testing included developing a procedure to fill and empty the device with oil from plastic containers so the oil could be reused. Finally, tests were run on dry specimens with the silicone oil. The results of two tests can be seen in Chapter 5.

Chapter 4 Experimental Methods

The tests reported herein were performed on dry Ottawa 20-30 sand because of the availability of comparative data in the literature. All specimens were prepared using dry pluviation to ensure spatial uniformity. A rectangular mold, sieve, and diffuser were used to evenly pluviate the particles, as seen in figure 4.1 and figure 4.2. The mold was slowly raised so that the drop height was kept constant. Final specimen dimensions were nominally 140 mm × 80 mm × 40 mm.

Figure 4.1 Rectangular pluviator for the preparation of cohesionless specimens.

Figure 4.2 One example of a sieve and diffuser set inserted into the pluviator.

Specimens were confined by using a vacuum applied to the top and bottom of the specimen or compressed silicone oil. If the specimens were confined with vacuum, the interfaces between the sidewalls and membrane were lubricated with Unisilikon, a silicone grease commercial lubricant. Specimens confined with silicone oil did not have the grease applied to the interface. All specimens were sheared at approximately 9 percent per hour (0.2 mm per minute). Detailed test procedures are presented in the Oregon State University Biaxial Manual in Appendix A, which has been modified from the procedure document developed at the University of Southern California (Rechenmacher 2017).

Chapter 5 Experimental Results

5.1 Overview

Table 5.1 summarizes the production tests performed with the device and comparative tests from the literature using a similar device.

Table 5.1 Summary of tests

Test Index	Relative Density (%)	Confining Stress (psi)	Confining Method	Test Location
V-1	65	10	Vacuum	OSU
V-2	56	10	Vacuum	OSU
S-1	43	20	Silicone oil	OSU
S-2	16	10	Silicone oil	OSU
BT-2030-07	39	10	Compressed air	Georgia Tech[a]
BT-2030-16	77	10	Compressed air	Georgia Tech[a]

[a] From Evans (2005).

5.2 Test V-1

The purpose of test V-1 was to troubleshoot the specimen and initial data acquisition set-up. The wiring for the LVDT channels was found to be incorrect in this test. As a result, only the axial LVDTs showed measurable change and had incorrect scaling. Therefore, the calculated axial strain for this test was smaller than the actual strain. Also, the precise axial strain at which shear banding initiated and the total volumetric strain were unknown for this test. However, the results showed the behavior of the axial and intermediate loads during the test. Figure 5.1 shows the specimen at the end of the test on the plane of zero strain. A shear band is visible.

Figure 5.1 Shear band from end of test V-1

This test was on a dense specimen with low confining pressure. The results were expected to be comparable to those of BT-2030-16. Dense specimens under low confining pressures are expected to dilate and exhibit strain softening. Such behavior is seen clearly in figure 5.2. The mobilized friction angle peaked and then gradually approached a constant at high strains (i.e., critical state). The peak strength in test BT-2030-16 was slightly higher than that in test V-1, which was expected because of the higher relative density in the former. Both tests exhibited a critical state friction angle of approximately 25°.

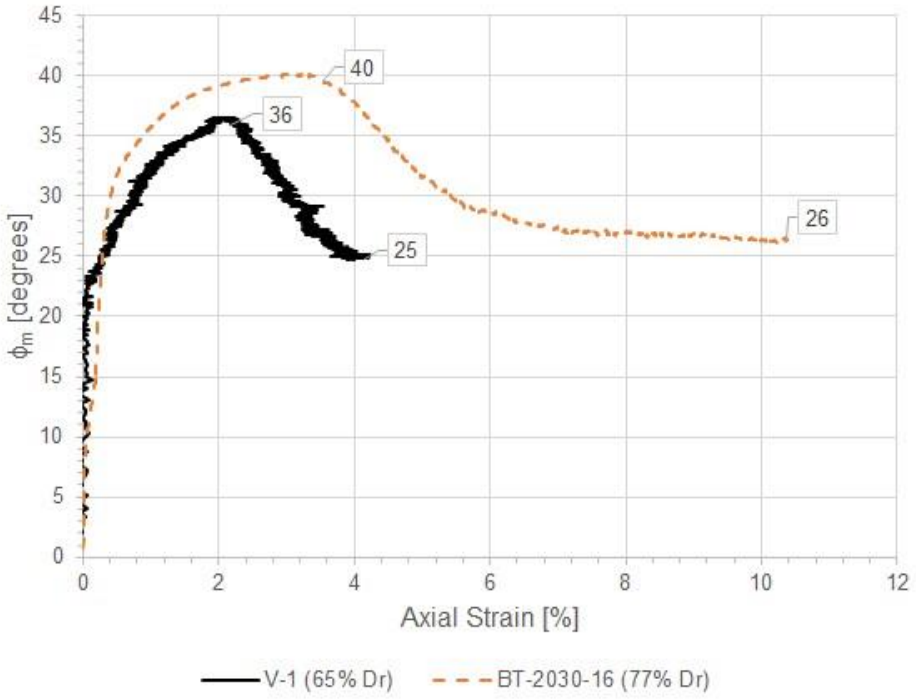

Figure 5.2 Mobilized friction angle of dense specimens with 10 psi confining pressure. Note the incorrect scaling of axial strain for test V-1.

5.3 Test V-2

Test V-2 was similar to test V-1 except that the displacement transducer wiring was corrected. The axial LVDTs lost platen contact soon after the onset of strain localization, causing the axial strain calculations to level out upon contact. The results are therefore presented with respect to time to fully show the behavior at high axial strain.

In comparing the relative density of tests V-2 and BT-2030-07, the friction angle of BT-2030-07 should be lower than that of test V-2. However, in figure 5.3 and figure 5.4, the opposite is seen. The friction angle of test V-2 approached 20°, while the angle of test BT-203007 approached 30°. Qualitatively, the agreement between tests was good, however.

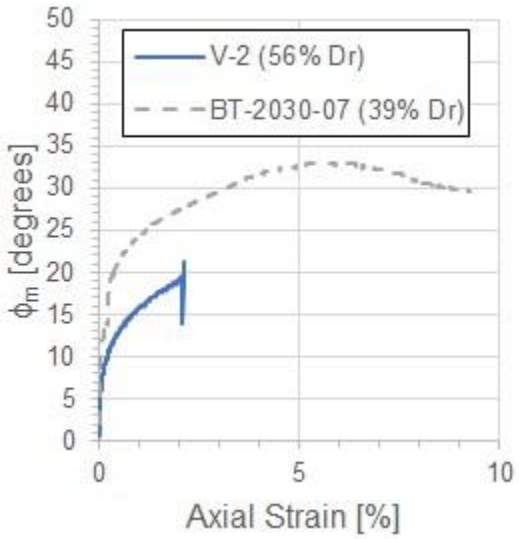

Figure 5.3 Mobilized friction angle of loose specimens with low confining pressure

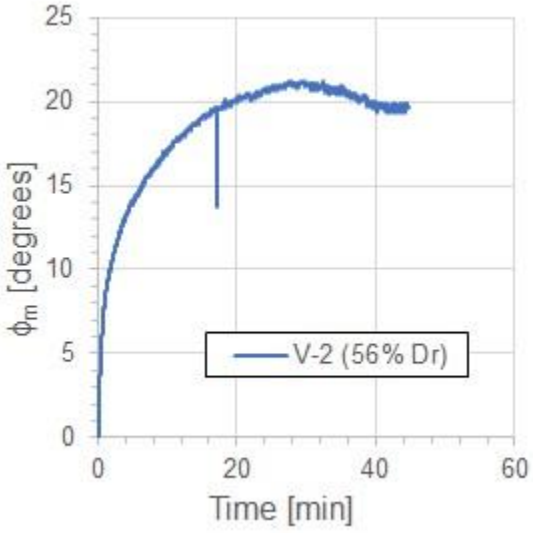

Figure 5.4 Mobilized friction angle of test V-2 with respect to time

A comparison of the axial load measured at the top and the bottom of the specimen is presented in figure 5.5. The axial load trend was similar to the load measured on the bottom load cells. Figure 5.6 shows that little force was measured on the top half of the constraining wall throughout the test. Therefore, the specimen wasn't contacting the constraining walls uniformly.

In conclusion, the axial load applied to the top of the specimen was transferred to the bottom of the specimen, but the specimen was tilted. This may explain why the friction angle for test V-2 was much lower than expected.

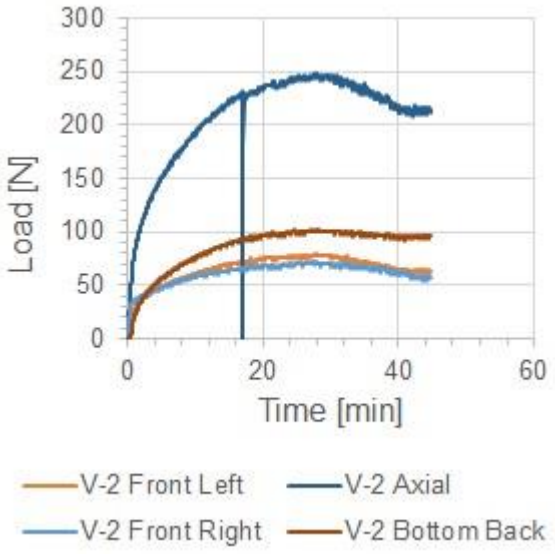

Figure 5.5 Axial loads measured in test V-2

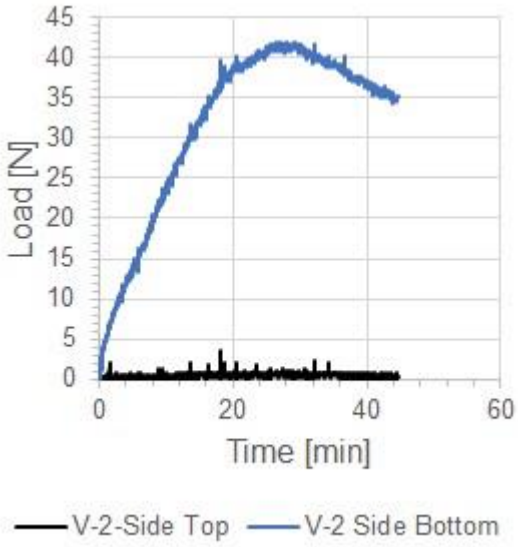

Figure 5.6 Side wall loads measured in test V-2

5.4 Tests S-1 and S-2

Tests S-1 and S-2 were performed with silicone oil used as the confining fluid. The tests were categorized as low density specimens with low confining pressures. The results were expected to be similar to those of BT-2030-07. Test S-1 was terminated before a visible shear band formed, so few of the post shear band data were captured. In Test S-2, the specimen fully compressed the front top LVDT. Therefore, sled displacement was restricted after the first band formed. This resulted in a second shear band forming as seen in figure 5.8. This as consistent with the behavior observed in specimens that had constrained sled movement reported by Alshibi et al. (2003).

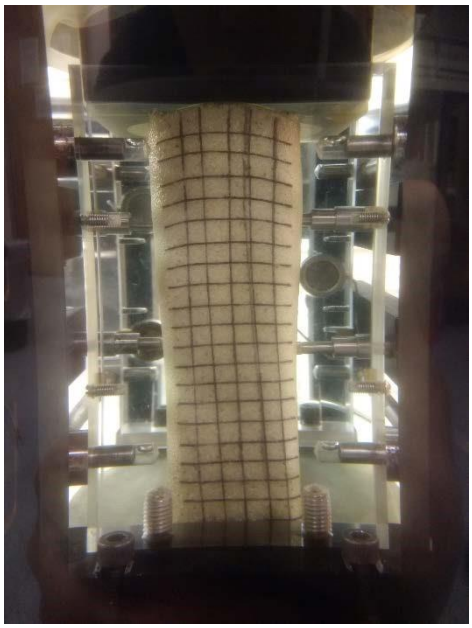

Figure 5.7 Test S-2 pre-shear looking in the direction of no strain

Figure 5.8 Test S-2 post-shear looking in the direction of no strain with two shear bands

As seen in figure 5.9, tests S-1 and S-2 showed strain hardening behavior with the friction angle approaching approximately 30° at high strains. Test BT-2030-07 showed slight strain softening but nonetheless had approximately the same friction angle at high strains. This as due to the slightly higher relative density of that specimen. Note that high strain behavior for Test S-1 could not be evaluated because of early termination of the test. The mobilized friction angle appeared to be similar to that of S-2 at low axial strains, but the same could not be confirmed at high axial strains. While the relative densities of the specimens varied, the friction angles at high strains on the failure plane approached the same value of 28°, as seen in figure 5.10.

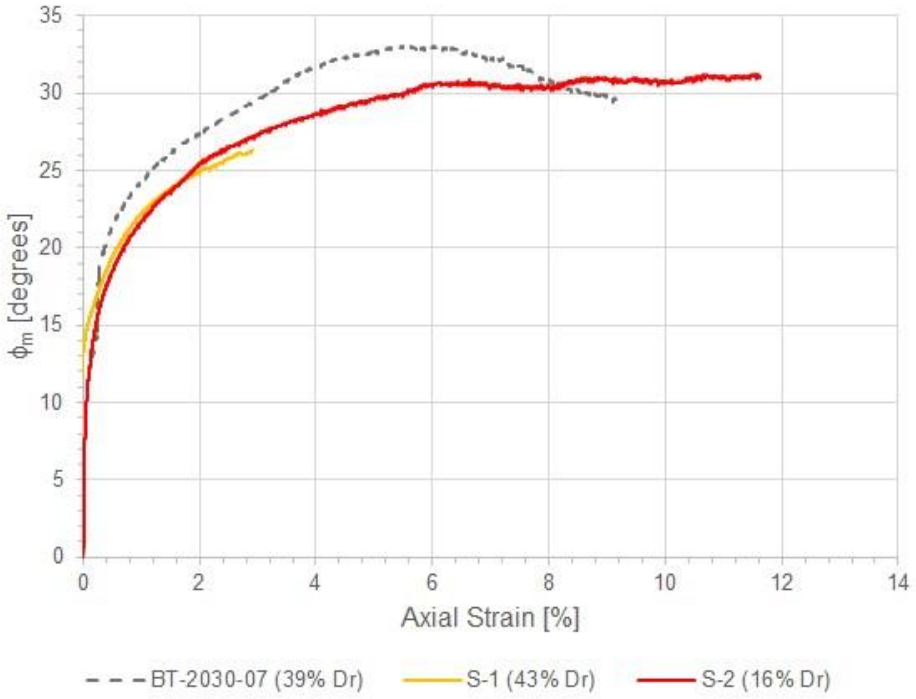

Figure 5.9 Mobilized friction angle of loose specimens

5.5 Friction

The effects of the lubricant used on the interface of the membrane and side walls can be seen in figure 5.10. Tests performed under vacuum, V-1 and V-2, had silicone grease on the interface. Tests run with silicone oil as the confining fluid, S-1 and S-2, had no additional grease on the interface. The figure shows that the friction for tests lubricated with silicone grease had lower overall system friction. This was due to the difference in viscosity of the confining fluids and lubricant. For tests V-1 and V-2, the silicone grease was surrounded by air. For tests S-1 and S-2, the entire cell was filled with silicone oil, meaning there was no difference in viscosities at the interface. This also confirms that the load cells had been set up correctly.

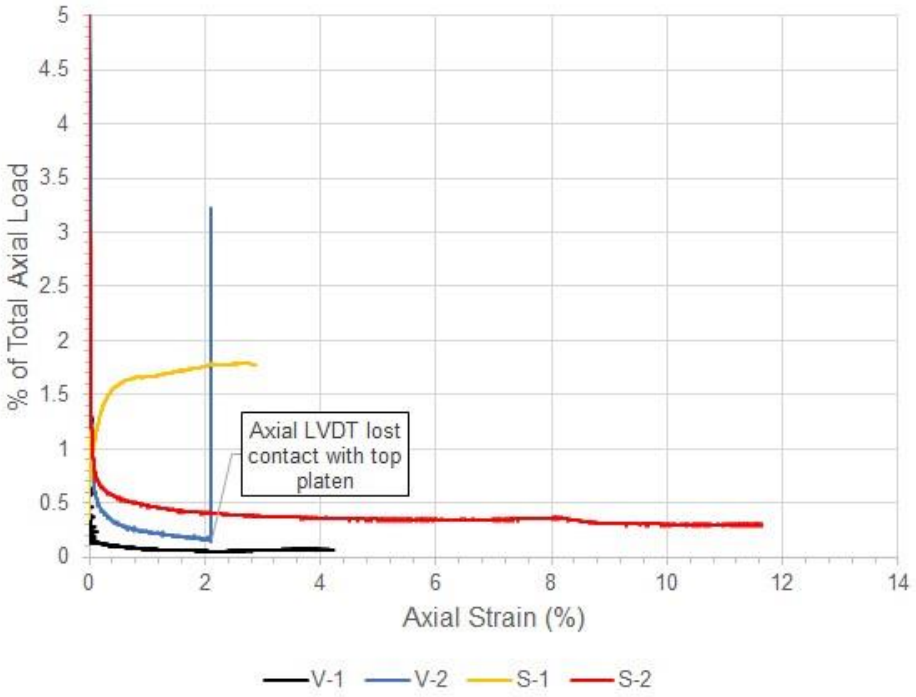

Figure 5.10 System friction for tests conducted at OSU

Chapter 6 Conclusions and Recommendations

Plane strain compression loading conditions are present in many transportation-related geostructures, such as long embankments and retaining walls. Soil behavior and strength are highly dependent on loading conditions. Yet, the design of those geostructures seldom characterizes soil by using those conditions. This is due to the rarity and expense of biaxial devices. A good understanding of soil behavior is essential for designing transportation geostructures. The work done in this project can now assist with that understanding.

The device was acquired "used" and "as-is," and there was significant effort in developing, installing, and testing the device. The device is now fully functional for testing dry soils. The results in Chapter 5 showed that qualitatively, the formation of shear bands can be observed. Quantitatively, the results were comparable to the tests conducted on the same material in Evans (2005). The automated data acquisition system is also functional and allows large amounts of data to be recorded with little effort. Clear procedures for testing and data recording have also been created for future use. The silicone oil can be used to conduct tests on saturated specimens, but additional equipment and LabVIEW coding are necessary. Nonetheless, tests on dry soils still offer valuable insight into the complex behavior of soils in plane strain compression loading conditions.

References

Alshibli, K. A., Batiste, S. N., and Sture, S. (2003) “Strain localization in sand: plane strain versus triaxial compression.” *Journal of Geotechnical and Geoenvironmental Engineering*, 129(6), 483-494.

Alshibli, K. A., Sture, S., Costes, N. C., Frank, M. L., Lankton, M. R., Batiste, S. N., and Swanson, R. A. (2000). "Assessment of Localized Deformations in Sand Using X-Ray Computed Tomography." *Geotechnical Testing Journal*, 23(3), 274-299.

Alshibli, K. A., and Sture, S. (2000). "Shear band formation in plane strain experiments of sand." *Journal of Geotechnical and Geoenvironmental Engineering*, 126(6), 495-503.

Arthur, J. R. F., Dunstan, T., Al-Ani, Q. A. J. L., and Assadi, A. (1977). "Plastic deformation and failure in granular media." *Géotechnique*, 27(1), 53-74.

Bolton, M. D. (1986). "Strength and dilatancy of sands." *Géotechnique*, 36(1), 65-78.

Cho, G. C. (2001). "Unsaturated Soil Stiffness and Post-Liquefaction Shear Strength." Ph.D. Thesis, Civil and Environmental Engineering, Georgia Institute of Technology, Atlanta.

Cornforth, D. H. (1964). "Some experiments on influence of strain conditions on strength of sand." *Géotechnique*, 14(2), 143-167.

Coulomb, C. A. (1773). "On an application of the rules of maximum and minimum to some statistical problems, relevant to architecture." *Mémoires de Mathématique & de Physique, présentés a l’Académie Royale des Sciences par divers Savans, &lus dans ses Assemblées*, Paris, 343-382.

Desrues, J., Chambon, R., Mokni, M., and Mazerolle, F. (1996). "Void ratio evolution inside shear bands in triaxial sand specimens studied by computed tomography." *Géotechnique*, 46(3), 529-546.

Dodds, J. (2003). "Particle Shape and Stiffness - Effects on Soil Behavior," M.S. Thesis, Georgia Institute of Technology, Atlanta.

Drescher, A., Vardoulakis., and Han C., 1990 “A Biaxial Apparatus for Testing Soils,” *Geotechnical Testing Journal*, 13(3), 226-234.

Evans, T. M. (2005). “Microscale physical and numerical investigations of shear banding in granular soils.” Ph.D. Thesis, Georgia Institute of Technology, Atlanta.

Evans, T. M., and Frost, D. (2010) “Multiscale investigation of shear bands in sand: physical and numerical experiments” *International Journal for Numerical and Analytical Methods in Geomechanics*, 34(15), 1634-1650.

Han, C., and Drescher, A. (1993). "Shear bands in biaxial tests on dry coarse sand." *Soils and Foundations*, 33(1), 118-132.

Han, C., and Vardoulakis, I. G. (1991). "Plane-strain compression experiments on water saturated fine-grained sand." *Géotechnique*, 41(1), 49-78.

Henkel, D. J., and Wade, N. H. (1966). "Plane Strain Tests on a Saturated Remolded Clay." *Journal of the Soil Mechanics and Foundations Division, ASCE*, 92(SM6), 67-80.

Kjellman, W. (1936). "Report on an Apparatus for Consummate Investigation of Mechanical Properties of Soils." *First International Conference on Soil Mechanics and Foundation Engineering*, Vol. 2, Cambridge, MA, 16-20.

Lade, P. V., and Wang, Q. (2001). "Analysis of shear banding in true triaxial tests on sand." *Journal of Engineering Mechanics*, 127(8), 762-768.

Lee, K. L. (1970). "Comparison of Plane Strain and Triaxial Tests on Sand." *Journal of the Soil Mechanics and Foundations Division*, 96(3), 901-923.

Nova, R. (2004). "The role of non-normality in soil mechanics and some of its mathematical consequences." *Computers and Geotechnics*, 31(3), 185-191.

Rechenmacher (2017). *Personal communication.* Oregon State University, Corvallis, OR.

Roscoe, K. H. (1970). "The influence of strains in soil mechanics." *Géotechnique*, 20(2), 129170.

Rowe, P. W. (1969). "Relation Between Shear Strength Of Sands In Triaxial Compression Plane Strain And Direct Shear." *Géotechnique*, 19(1), 75-86.

Terzaghi, K. V. (1936). "The shearing resistance of saturated soils." *Proceedings of the First International Conference on Soil Mechanics*, Vol. 1, Cambridge, 54-56.

Vardoulakis, I. (1996a). "Deformation of water-saturated sand: I. Uniform undrained deformation and shear banding." *Géotechnique*, 46(3), 441-456.

Vardoulakis, I. (1996b). "Deformation of water-saturated sand: II. Effect of pore water flow and shear banding." *Géotechnique*, 46(3), 457-472.

Vardoulakis, I. (1980). "Shear band inclination and shear modulus of sand in biaxial tests." *International Journal for Numerical and Analytical Methods in Geomechanics*, 4(2), 103119.

Vermeer, P. A. (1990). "Orientation of shear bands in biaxial tests." *Géotechnique*, 40(2), 223236.

Yoshida, T., Tatsuoka, F., Kamegai, Y., Siddiquee, M. S. A., and Park, C. S. (1994). "Shear banding in sands observed in plane strain compression." *Proceedings of the 3rd International Workshop on Localization and Bifurcation Theory for Soils and Rocks*, Rotterdam, 165-179.

Yoshida, T., and Tatsuoka, F. (1997). "Deformation property of shear band in sand subjected to plane strain compression and its relation to particle characteristics." *Proceedings of the*

14th International Conference on Soil Mechanics and Foundation Engineering, Hamburg, 237-240.

Appendix A OSU Biaxial Testing Procedure

BIAXIAL Testing Apparatus

Test Procedure

Geotechnical Engineering Laboratory
Oregon State University
Dr. T. Matthew Evans

Modified from original provided by Dr. Amy Rechenmacher
Granular Mechanics Imaging Laboratory
University of Southern California

Table of Contents

Biaxial Manual: Introduction

Running a biaxial test is a delicate procedure that requires attention, time and patience. Expect to be in the lab for no less than a two day period. Two critical things determine how much time the test takes: the shearing rate and the primary saturation time.

Major steps in running a biaxial test

1. Set valves to initial positions (see below).
2. Fill burette reservoir with de-ionized, de-aired water.
3. Prepare lab for test, perform pre-test
4. Prepare sample
5. Assemble the biaxial apparatus
6. Fill cell with oil
7. Place loader
8. Initialize motor and record sensor reading
9. Primary saturation
10. Back pressure saturation and b-value check (typ. overnight)
11. Consolidation
12. Shear (time depends on shearing rate) 13. End test and empty oil from cell
14. Disassemble cell and specimen.
15. Clean the lab

Filling Burettes with De-aired water

1. Make sure house de-aired water is connected to the burette panels and turned on.
2. Make sure the following valves are closed:
    a. Valves 5 and 6, Left and right small burettes
    b. Valve 9, Reservoir
    c. Valve 10, Combined burette
    d. Valve 11, Pressure Control, on vent
3. Open: Valves 7 and 8, Left and right big burettes
4. Turn Valve 9, “Reservoir” to “Fill Burette” position.
5. Slowly open Valve 10, “Combined burette”, to “Fill Burette” position.

6. Burettes should start filling.
7. Close Valves 9 and 10 when burettes are full to desired height. DO NOT OVERFILL THE BURETTES ABOVE THE MARKED SCALE!
8. Note the following:
    a. Burettes can be filled separately or combined.
        i. Two big burettes, Open valves 7 and 8 and close 5 and 6. ii. Small burettes, open valves 5 and 6 and close 7 and 8.
        iii. Individual burette, open respective valve and close others.
    b. Small burettes are very sensitive and must be filled *EXTREMELY SLOWLY*. They are typically not used in the biaxial tests because of this.

Pre-test procedure (to be done the "day before" the test)

1. Make sure all apparatus parts are available and have them ready for use:
    a. Top and Bottom Platens
    b. Axial Rod and collar
    c. Two glass walls and two plexi-glass walls
    d. Two screws to fasten walls to biaxial base
    e. Four screws to fasten axial load cell to top platen
    f. Four adjustable fasteners (tie rods)
    g. Four screws and 2 brass fasteners for EACH sidewall
    h. Two large nuts to secure axial loader
    i. Four O-rings (top and bottom platens)
    j. Four base plate screw rods (large and tall, threaded at ends).
    k. Two sled breaks
    l. Four (each) top plate nuts and washers
    m. Axial loader guide pin and 2 screws
2. Determine which material will be used for the test, and make sure you have enough material to perform the test. Guidelines for masses needed for dense specimens are given on the table on page 8. Oven dry the material for at least 12 hours (if not already done).
3. Drain all the water from top and bottom drainage specimen lines that remained from previous test. Fill big burettes with de-aired and de-ionized water.

4. Make sure all internal sensors are connected to the biaxial base and that all are working (meas + automation: test sensors). Check "zero" points: if not zeroed, adjust scale intercepts using National Instruments (NI) Measurements and Automation (M&A) software.
5. Select and clean a biaxial membrane and "water test" *thoroughly* to check for holes (if not already done). Dry well using paper towels and store away from light. If membrane is damaged, do not use it (but save it for use for platen membranes).
6. If platen lubrication is desired:
    a. Cut top (square) and bottom (circular) platen membranes. Use a triaxial membrane (preferred because typically thinner) or a discarded biaxial membrane. Lay the paper templates over the membranes, outline the template marker, then cut out the membrane, cutting *out* the marker lines (else membrane will be too big for the platens or may block porous stone openings. Store cut membranes in the drawer until ready to use.
7. Wipe glass and Plexiglas sidewalls using Kim-wipes only. *Do not use paper towels, as they can scratch the glass!!*
8. Write (with thick Sharpie marker) the test number on the *specimen side* of the glass walls (side where cross hairs are etched). Also, with a thin Sharpie marker, mark the cross hairs prominently (used for image scaling).
9. Cut filter paper rectangles for top and bottom platens (size to generously cover porous stones, about 2/3 of specimen cross-sectional area).
10. Flush platens with water to examine if clogged: Connect platen to de-aired water supply. Water should flow freely through the porous stone. If clogged, boil stones for 10 min. and/or soak in vinegar.
11. Blow compressed air through the top and bottom drainage lines in the biaxial base to remove water.
12. Clean glass portion of platens and Plexiglas and glass sidewalls with Kim-wipes (DO NOT use paper towels to dry the platens, as they may scratch the glass).
13. If platen lubrication is desired:
    a. Be sure enough Unisilkon: Klubber paste lubricant mixture is prepared. The lubricants should be mixed in a ratio of 5(big):1(small).
14. Have mold ready and clean with accessory hoses.

15. Have o-rings ready and clean.
16. Have needed tools ready:
    a. Brushes, Picture 3
    b. Calipers
    c. Dishes
    d. Specimen preparation devices (funnel, pluviator mold, screens, etc)
    e. Kimwipes
    f. Mold vacuum hose
    g. Notebook, data recording sheets, and Pen
    h. Scissors, Picture 1
    i. Spoons, Picture 1
    j. Many, many, MANY paper towels
    k. Vacuum grease, Picture 2
    l. Wrenches:
        i. Allen/Hex: 1/4, 3/16, 5/32, 9/64
        ii. ½ – 9/16, ½ – 7/16, 7/16, 9/16, Adjustable
17. Drain all the water from top and bottom drainage line that remained from previous test.
18. Clean counter and create space to work
19. Retract motor Shaft by removing guide pin plate and screwing the shaft upwards.
20. Clean the axial rod in the top plate and apply Teflon grease. Position the axial rod in the all the way up in the plate. Tighten in place.
21. Loosen circular axial rod bushing above the black cross beam in biaxial internal frame.
22. Replace oil drainage caps under apparatus.

Biaxial Test Procedure:

Specimen mold preparation

1. Remove sand from oven. Allow the porcelain dish to cool completely. Cover sand with paper towels to prevent dust/moisture contamination.
2. Trim ends off of biaxial membrane (remove only the end circular part; leave as much "freeboard" as possible to wrap ends of the membrane up and around the specimen mold.
3. Measure and record the thickness of the biaxial membrane with the calipers (check both bottom and top). Typical thickness is around 0.4 mm.
4. If platen lubrication is desired:
    a. Put a *thin* layer of Klubber lubricant (5:1 mixture) on bottom platen. Grease should be thin enough to provide lubrication, but not too thick to squeeze out from underneath the membrane. *Make sure no grease gets on the porous stone!*
    b. Place platen membrane (circular for bottom platen) on the lubricated platen. Remove as many air bubbles from under the membrane as possible. Flip the membrane, pat down to fully lubricate, then reverse back to original side and again remove all air bubbles.
    c. Repeat steps 4a-4b for top platen. Also, put thin layer of lubricant around side rectangular edges to provide for easier insertion into mold.
5. Put a fairly thick layer of vacuum grease in the o-ring groove around the perimeters of both platens. Fill in the O-ring groove completely.
6. Configure the mold with the 2-pronged hose connector.
7. Connect the vacuum pump to the mold.
8. Place membrane inside mold (square end is top). Try to have membrane as much in position as possible.
9. Wrap the ends of the membrane around the top and bottom of the mold.
10. Turn vacuum pump on and increase vacuum pressure to about -10 to -20 kPa (3 inHg to 6 inHg).
11. Adjust the membrane in mold so it fits *perfectly*. This WILL take time, so be patient. It is especially important that the membrane corners are aligned with the mold corners. If adjustment is difficult, reduce the pressure (the higher the vacuum pressure, the harder it is to adjust.)

12. Once the membrane is in place, increase pressure to -40kPa (~ 12 inHg).
13. Invert the mold. Place the circular bottom platen (upside down) on the mold: the water plug in bottom platen should be perpendicular to one of the longer sides. Center the platen such that the mold edges align with the platen edges. Make sure the porous stone and specimen cross section are centered over the platen.
14. Fold the membrane around the bottom platen, being careful not to let the platen to get off center (especially if the platen is lubricated). Tug the membrane slightly to eliminate potential creases in the membrane between the platen and mold.
15. Carefully put one o-ring in groove and make sure the bottom platen is not moving. Make sure o-ring is in groove and tug upward on the membrane to eliminate all creases.
16. Put a second o-ring next to first to secure the seal.
17. check that the mold cross-section is centered around the bottom platen porous stone. If not, remove bottom platen and start again.
18. Carefully trim off excess membrane, leaving about 1 in. Fold membrane around platen. On the bottom platen, excess membrane can interfere with sidewall placement, so use extra care to trim excess there. Wipe excess grease off bottom of platen.
19. Carefully turn the mold right side-up without moving the bottom platen, and place the mold on a metal tray (the metal tray will be used as a means to later transfer the filled mold to the biaxial apparatus).
20. Place a rectangular shaped filter paper over the bottom platen porous stone.

Filling the mold with sand (via dry pluviation)

1. Weigh empty dish, then weigh dry sand + dish. Record respective masses in test notebook (two decimal places). **Target masses are: (for "dense" sand)**

Material	Target dry mass for "dense" specimen *	Pluviator withdraw rate	Mass of "extra" material needed for overfill
Glass beads (GBC)	770 g	4 mm/sec	~ 70-80 g
SC sand	760 g	3.33 mm/sec	~50 g
MC sand	745 g	5 mm/sec	~60 g

* for 13.5-cm drop height (corresponding to "100" mark on pluviator starting at 220 mark on Plexiglas) ← *check it is not the 50 mark!*

2. To fill mold with sand:

a. Mount acrylic confining pieces on top of mold (the ones with the written numbers and horizontal lines on them).
b. Prepare pluviator device with appropriate screen and opening plate. Place the long aluminum stick with duct tape on one end over the bottom openings.
c. Fill pluviator device with desired test material to about 2-3cm from the top (for tests on DENSE specimens: if more, you may overfill the specimen mold; if less, you may not have enough to fill mold.
d. **Have empty bowl ready and close to specimen mold, so that if mold becomes too full, the pluviator can be quickly withdrawn to let excess material fall into bowl.**
e. Have timer ready and ***know your pluviator retraction rate***. Release opener and fill mold, keeping drop height constant throughout filling.
f. Remove extra sand VERY gently and carefully, and return to dish. *Be careful not to lose sand: mass of remaining sand will be used to determine the mass of sand in the specimen!* It is helpful to "flick" excess sand to the mold "shoulders", and then "sweep up" the excess using a small brush and spoon. *It is very important that the final sand surface be level with the mold shoulders*. This is a very delicate procedure, so use care and patience. Scotch tape works well for sand but has too much static for glass beads.

3. Use a leveling tool to verify that specimen top surface is flush with mold "shoulders" (Picture 10 Sand flush with mold).
4. Collect any excess sand spilled in an around specimen and return to dish. Weigh the remaining sand + dish. Subtract from that the initial mass of (sand + dish) = mass of dry sand in the specimen. Record value in test notebook.
5. Place a rectangular-shaped filter paper centered over the specimen top surface.
6. Place top platen carefully, with water port oriented 180 degrees from bottom platen port.
7. Fold membrane around top platen while holding the mold in place.
8. Place o-ring in grove. Make sure the bottom platen does not move when placing o-rings.
9. Place a second o-ring below the first o-ring to secure sealing.
10. Cut excess membrane from top, leaving ~1.5 in. Make sure no sand grains or vacuum grease are blocking either drainage port. Wipe excess vacuum grease off platens.
11. Carefully bring the mold on the metal tray to the biaxial device (using metal tray helps ensure that the bottom platen does not become detached from the mold, causing sand to spill out

between mold and bottom platen). Orient so that the bottom drainage port pointing away from the apparatus. Make sure the vacuum lines do not become tangled.

12. Reduce cacuum pressure to zero and disconnect vacuum hoses from mold. Disconnect the 2pronged vacuum hose connector from vacuum pump and return promptly to storage.
13. Make sure drainage lines inside the cell do not have water in them. If they do, blow compressed air through the lines to clear.
14. Connect top and bottom drainage tubes (inside the cell) to top and bottom platen ports. Bottom platen line should be the front-most line. Thread the top platen drainage line (coming from back) between the two split columns. *Be sure to connect the lines such that they will not get tangled with other hoses/wires when specimen is placed in the cell!*

Biaxial apparatus assembly procedure

1. Raise the black cross beam in internal biaxial frame as high as possible to create clearance for specimen placement.
2. Move the sled as far forward as possible. *Note: the "back" of the apparatus is the side where all the electrical cables exit the cell!*
3. Close the bottom drainage port outlet (in biaxial base) with a cap.
4. Connect the vacuum pump line to the top platen drainage port outlet on biaxial base.
5. Turn vacuum pump on to -40kPa (12 inHg) or to a value lower than the desired final confining stress.
6. Slowly and cautiously remove mold, *removing both sides of the mold at the same time*, trying not to disturb the specimen.
7. Measure the specimen width and length at three different places: mid-height and ~1-2 cm from the top and bottom. Record these measurements. Width and length will be the average of the 3 measurements, minus 2x the membrane thickness. Specimen height is difficult to measure accurately, so use (mold height = 139.7 mm):

   Height = {139.7 + [2 x (membrane thickness)]} mm
8. **Start the Labview program**. Run "Biax 3.0.vi" and follow the code prompt in parallel to the procedure below:
   a. Choose the directory and *filename prefix* where the data will be stored (or else test won't proceed).

b. Fill in the specimen height, length and width, and *filename prefix.*

9. After filling in all necessary information, click OK. Code should now be displaying a window showing all sensor readings.
10. Cautiously lift specimen by the bottom platen and place it on sled (bottom platen drainage port facing front and top drainage port to the back. Make sure the o-ring is still in groove.
11. Cut or tuck extra membrane around the bottom platen in order not to interfere with the eventual placement of the sidewalls.
12. Make sure the load cells are inside the load sidewall, with their backs facing the glass wall and their tips on the metal part inside the Plexiglas. Plug side wall load cells in.
    a. Side Top CH6
    b. Side Bottom CH4
    c. Side Middle CH5
13. Make sure the sidewalls are clean. Re-wipe with Kimwipes if necessary
14. Connect the glass and Plexiglas walls: place the walls together, and then screw in the fasteners. *Do NOT slide the glass across the Plexiglas!* Make sure crosshairs are on outside of glass (not touching Plexiglas).
15. Lubricate short sides of the specimen and glass walls *VERY* thoroughly with silicon oil. If low system friction is desired, silicone grease (Unisilkon) can be used instead. However, the grease is not suitable is pictures shall be taken for image processing since it clouds the side of the specimen.
16. Lubricate the sled shoulders and wall bottoms with silicone so walls slide in position easily.
17. Place load-cell sidewall so that it contacts the specimen uniformly, both vertically AND horizontally – *THIS IS VERY IMPORTANT!!!!* Use the sidewall readings in the Labview program that the specimen uniformly touches the load-cell sidewall.
18. Place second sidewall and make sure it contacts the specimen uniformly.
19. Fasten the load cell wall to the biaxial base using the 2 hex screws. Do not tighten second glass wall to sled yet! Re check that the sides of the sample are parallel to glass walls (you can rotate the sample to do this).
20. Center the sled and glass walls for picture taking. Put on sled breaks and tighten.
21. Lower black cross bar until load cell rests on top platen. The cord from the load cell should come from the front left at 45°. Loosen axial rod break, loosen the axial rod bushing (if not

loose already), and re-raise black cross bar to allow space to screw load cell to top platen. Tighten axial load cell firmly in place using 4 hex screws (large). Be careful not to torque the specimen while tightening.

22. Place adjustable sidewall fasteners. Try to tighten in parallel. Loosen or tighten fasteners so that the specimen uniformly contacts the wall and load cells are reading comparable positive values (wall should be as uniformly loaded as possible).
23. Fasten the second sidewall to the biaxial base using 2 hex screws.
24. Using the screw at the top, lower the rectangular black cross beam as much as possible. (about ¼ - ½ inch clearance between top of load cell and bottom of cross bar.)
25. Push down slightly on the axial rod to read the bottom platen load cells. Shift the bushing (i.e metal collar around axial rod) until load cell readings are approximately uniform. Verify by eye that the specimen is oriented vertically and not tilting. ***Tighten bushing and axial rod break***.
26. Place axial LVDT holders: they attach to the top rectangular plate, and both fasten on the side nearest the computer (left side, standing in front of apparatus). Position the axial (long) LVDTs on the edge of the top platen, located diametrically opposite from each other. Set LVDT's to read about -10 mm (-12.5mm < LVDT < +12.5mm) if running a compression test (a "-" reading means LVDT is compressed beyond half way).
    a. Axial Front CH0, No. 54107
    b. Axial Back CH1
27. Fasten the 4 side LVDT holders to the either the BACK or FRONT split column. The LVDT holder is connected to the correct split column if the tightening screw is oriented up. Make sure the copper shims are in place to prevent damaging the column. Position LVDT's in the holders to read > +1mm (-6mm < LVDT < +6mm). Make sure opposite LVDT pairs are at approximately the same height. To have room to fasten LVDT's to their respective holders, place LVDT in the following order:
    a. Front Bottom CH2, No. 56337
    b. Front Top CH3, No. 56341
    c. Back Bottom CH4, No. 56340
    d. Back Top CH5, No. 56338
28. Place the sled LVDT on back. (CH6, no. 56339). Position carefully so as not to obstruct eventual sled movement (allow ~5 mm clearance, or +1 mm setting).

29. Wrap black electrical tape around the LVDTs to prevent reflections in the images.
30. Once all sensors are in position, click “Done”.
31. Make sure once again that the o-rings are in the platen grooves.
32. Make sure sled “skirt” is in place.

Placement of cell

1. Tie electric wires together so that they are out of the way and do not interfere with imaging or cell placement (not touching the biaxial base o-ring). *Leave drainage lines free and untied*.
2. Record sensor readings.
3. Lubricate the biaxial *bottom* o-ring with silicon oil.
4. Use Kim-wipes to clean the Plexiglas cell *again*.
5. Unlock the axial rod break *inside* the cell.
6. Carefully lower the cell in place. Make sure wires and drainage lines do not interfere with view through the imaging windows or base o-ring seal.
7. One or two people should lift the cell. Apply homogenous pressure down on the top of the cell to seal it around the bottom o-ring.
8. Twist the cell left and right to make sure the o-ring is fully lubricated.
9. Screw the 4 vertical top-plate support rods into the biaxial base.
10. Slowly remove sled breaks (if appropriate): first, loosen breaks, both at the same time; then, remove breaks one at a time.
11. In the cell top plate, make sure the axial rod is all the way up and tightened, excess grease has been cleaned, the rod freshly greased (Teflon grease ONLY!), and the air outlet port is open.
12. Place the top plate on cell cautiously, with the air inlet open and pointing to the front.
13. Apply homogenous pressure downward on top plate (do with 2 people) to seal o-ring.
14. Place rubber washers and nuts on the rods and tighten the nuts firmly and uniformly. Diagonal nuts should be tightened at the same time.
15. Holding the axial rod, loosen its break, and gently lower the axial rod to just barely touch the internal axial rod (Picture 13 Top platen rod and internal axial rods). Re-tighten the axial rod break firmly.

Mounting the Axial Loader

1. Place loader mounts (black, 12-in.-tall things) over the threaded rods in the top plate.

2. Unscrew and remove aluminum axial guide from the loader (3/16 hex wrench).
3. Manually rotate and retract the axial shaft (Picture 7 Motor shaft) to its highest position so that it does not "bump" the axial rod during placement of the loader.
4. Slowly place motor in position over the loader mounts on top of the biaxial top plate. As the sled is unlocked and very sensitive to movement, try to minimize disturbance to the cell and specimen.
5. Manually advance (by rotating) axial shaft to make sure it is properly aligned with the axial rod. If it is not, adjust lateral loader position. Continue to rotate motor axial shaft so that the motor shaft and axial rod are connected over ~ ¾" length.
6. Place nuts and fasten motor in place. Use a wrench to tighten nuts.
7. Replace aluminum axial guide on bottom of loader, making sure pin is aligned in the groove.
8. Tighten the motor axial shaft screws securely to the axial rod.
9. Connect motor electric wires.
10. Unscrew and loosen *external* axial rod break.
11. **Turn motor on** *(motor must warm up for at least 5 min., and it will be used in next step).*
12. Slowly and carefully move biaxial table to final test position. Secure table feet to floor. Use a level to level table.
13. Click OK on Labview code to proceed with filling the cell with oil.

Filling Cell with Oil

1. Close the air inlet valve and connect a regulated vacuum source.
2. Place a small bowl below the bottom front of the cell and connect the oil hose (quick-connect connecter) to the bottom front of cell.
3. Make sure oil drainage caps under apparatus are in place and tight.
4. Place one open end of oil drainage line into a full container of silicone oil.
5. SLOWLY increase vacuum pressure to -35 kPa (~10.3 inHg). It's best to increase and wait, since it takes a while for the vacuum pressure to become steady. Open the air inlet valve. OPEN the oil hose valve at the bottom front of the cell (valve pointing toward the oil tubing line = open). Oil should start flowing into the cell.
    a. *Do not increase cell vacuum pressure to a value higher than specimen pressure. This would remove the vacuum from the specimen and cause the specimen to fall.*

b. The difference between the vacuum applied to the top of the cell and the vacuum applied to the specimen is the confining pressure on the specimen. If the difference becomes small, the specimen will start to deform.
c. If a faster filling rate is desired, slowly increase the vacuum on the specimen AND in the cell. Be sure to maintain at least a 15 kPa difference between the two.

6. Once one container is about to empty, follow these steps to switch to a full container:
    a. Close air inlet valve at top plate of cell.
    b. Close oil input valve at bottom of biaxial cell.
    c. Place open end of oil drainage line into a full container of silicone oil. Close the other nearly empty container to prevent oil contamination.
    d. Open air inlet valve at top plate and then open oil input valve at bottom of biaxial cell to continue filling.
7. Continue filling cell until only about 1-2 in. of air is left at the top. *Do not overfill*. Be sure that the specimen top platen is completely immersed in oil.
8. When cell is filled to desired level, close oil input valve at bottom of biaxial cell. Slowly reduce cell vacuum to zero.
9. Slowly open valve at top of the oil reservoir tank to release excess vacuum. When vacuum has fully dissipated, close valve.
10. Flush the oil lines of air bubbles: Open the oil valve at the front-bottom of the biaxial base. Have many paper towels handy! Unscrew the cap on top of the oil pressure transducer, and allow oil to drip until all air bubbles out of the oil lines. Replace the cap, then close the needle valve at the bottom of the cell.
11. Connect the cell pressure air supply line to valve coming from top of cell. Open valve.
12. Record all sensor readings.
13. Click “Done” on the Labview screen to proceed with initialization.

Initialization, application of initial confining pressure:

1. Click on the "Position Motor" button to position the motor shaft and follow the prompt (the motor will advance until a minimal [3 kg] load is registered by the axial load cell, ensuring that the axial rod is in contact with the top of the specimen.
2. The program will prompt the user once the load is achieved. Click OK to proceed.
3. Make sure Oil valve at the front of the biaxial base and air valve to top of cell are open.
4. Apply an initial confining pressure to the cell (typically ~ 40kPa).
5. Reduce and turn off the vacuum on the specimen. Remove vacuum line from top and bottom of specimen drainage line. Click "Done" on the screen and follow instructions.

Flushing the specimen with CO_2 (optional):

1. Connect CO_2 line and needle valve to bottom of specimen drainage port in biaxial base. Needle valve should be closed at this point.
2. Connect CO_2 verification hose (labeled CO_2 out) to top of specimen outlet in biaxial base. Place loose end in a jar of water (Picture 8).
3. Open CO_2 tank valve and *very slowly* increase CO_2 pressure to 2.5 psi (17 kPa). *Do not exceed 5.8 psi (40 kPa), else you might explode the specimen!*
4. Slowly open the needle valve. CO_2 should start to bubble out the top platen drainage line in the water beaker. If it does not, verify that the correct valves are opened. If CO_2 still does not flow, this means there is a clogged line somewhere.
5. Leave CO_2 running for at least 1 hour.
6. After 1 hour, slowly close the needle valve. Reduce CO_2 pressure to zero. Close CO_2 tank valve. Leave needle valve closed and in place, but remove CO_2 line from needle valve. Store CO_2 line near CO_2 tank.
7. Record all sensor readings.

Primary Saturation

1. Bleed differential pressure transducer on the burette panel (5/64" hex wrench): open burette valves 7 and/or 8, open the tiny screw on the side of the transducer, and allow water to drip out. Close screw and valves.
2. Make sure "big" burettes are full of de-aired water.

3. Remove air bubbles from **bottom** of specimen drainage line and attach line to inlet port in biaxial apparatus (where the CO_2 needle valve is now attached:
    a. Uncap bottom specimen drainage line and lay it next to the CO_2 needle valve.
    b. Open both burette valves (7 and 8) and set main burette Valve 10 "to sample".
    c. Open bottom of specimen valve, Valve 2 (top of specimen valve, Valve 3, should be closed). Water should be dripping from the end of the line. Allow water to drip until all air bubbles are out of the line.
    d. Loosen needle valve/CO_2 connection from bottom of specimen drainage port in the biaxial base. Remove it and *quickly* connect the dripping, bottom of specimen water line to this port (try to minimize air entry).
4. De-aired water should now be flowing by gravity through the specimen, but the process will occur slowly. Observe the burette water level to see if it is lowering.
5. In order to speed primary saturation, apply "back pressure" (bp) to the top of the burettes: Turn burette pressure valve, Valve 11, to "pressure". Slowly increase bp (knob 2) to 10 kPa but no more than 20 kPa. You should see the water level lowering in the burettes and rising within the specimen. If you do not, this means one of the drainage lines is clogged. Troubleshoot; else the test probably has to be terminated.
6. If needed, connect the vacuum pump line to the top of specimen outlet in the base of biaxial. Apply -20 kPa of vacuum pressure. Water should start flowing into the specimen more quickly.
7. Watch the water level in the burettes: *never* let them empty completely! When burettes are near empty, reduce vacuum pressure and bp to zero. Turn Valve 11 to "vent", close valve 2, turn valves 9 and 10 to "fill burettes". Refill burettes according to the procedure above. Close valves 9 and 10. Turn valves 10 to sample and open valve 2. Turn Valve 11 to "pressure". Increase bp and vacuum pressure as above.
8. Continue primary saturation until water is seen to reach the vacuum pump water reservoir (or water with no air bubbles comes out of outlet) and/or at least 3 pairs of burettes have drained into the specimen.
9. Once primary saturation is complete, reduce back pressure and vacuum pressure to zero. Turn Valve 11 to vent. Close valve 2 and 10.
10. Remove air bubbles from **top** of specimen drainage lines: (Do this while water from bottom is draining through!)

a. Uncap top specimen drainage line, and lay it next to the top of specimen outlet port in the biaxial apparatus base.
b. Open both burette valves (7 and 8). Set main burette Valve 10 "to sample".
c. Open top of specimen valve, Valve 3. Let the water drip.
d. Loosen the vacuum hose connected to top of specimen outlet in biaxial base and remove completely, and *quickly* connect the dripping top of specimen line to the top of specimen outlet, trying not to allow air bubbles to get into the hose.

11. **Remove air bubbles from pwp transducers** (one at a time): open valves 7, 8, and 10, open drainage lines 2 and 3, unscrew caps above transducers, let air bubbles escape, close caps securely.
12. Refill burettes to appropriate water levels in preparation for bp sat, consolidation, and shear. *Note, there is no way to "fill" the burettes after this point, because the water will be pressurized.* Water level should be chosen in anticipation of specimen volume changes expected during bp sat, consolidation, and shear. Specimens will take in water during bp sat (burette water level will lower); expel water during consolidation (burette level will rise); during shear, a dense sand will dilate (take in water, burette level will lower), and a loose sand will contract (expel water, burette level will rise). Plan burette water levels accordingly. *For dense specimens, set the burette level around 2/3 to 3/4 full!*
13. Close valve 8, open valve 7. Close R burette valve, only L burette used for BP saturation and consolidation.
14. Keep valves 2 and 3 open, valve 10 "to sample", to allow specimen water levels to equalize.
15. Press done on screen to continue to bp sat.
16. Record load cell/LVDT readings

Back Pressure Saturation and B Value Check

1. Turn Valve 11 to "pressure". Make sure valves 2, 3, 7 and 10 are open to "samples" and valve 8 is closed.
2. Begin Back Pressure Saturation in the Labview code. During this phase, the Labview code automatically adjusts cell confining pressure in response to manual back pressure changes to maintain the specified effective stress (typically 40 kPa).

3. Input desired effective stress level. Input a "delta effective stress" to be applied during a Bvalue check (typically 20 kPa). Both values can be changed later if needed. Click OK.
4. *Slowly* increase back pressure to 150 kPa. Cell pressure should adjust to maintain the specified effective stress.
5. Leave the stress increment for couple of hours (or overnight) to allow pressure to equalize through the specimen. Monitor water level in burettes.
6. Perform a B-value check. Press Start B-value button and follow the program prompt:
    a. Close drainage valve 2 and 3.
    b. The cell pressure will be increased $\Delta\sigma_{cell}$ = 20 kPa (or whatever value is specified). The corresponding increase in pwp will be measured by the pore pressure transducers (top and bottom). The B-value ($B = \Delta u / \Delta\sigma_{cell}$) will be calculated versus time. If the specimen is completely saturated (S = 1.0 or 100%), B = 1. If S<100%, B<1.
7. Allow the B-value check to run until B stablizes (~2-3 minutes). Once stabilized, click stop B-value button. Open valve 2 and 3. Record B-value.
8. A B-value of 0.95 or above is desired. If B-value is less than 0.95, increase bp by 50 kPa and repeat steps 5-7.

    Before class: Record burettes.

    After class: Record burettes, perform B-value check. 1 minute ate the check is over, slowly increase backpressure (bp) to 225 kPa. Record burettes and leave overnight.
9. Stop back pressure saturation when B > 0.95 OR cell pressure is less than 650 kPa minus the desired final effective stress at the end of consolidation (the cell capacity is 650 kPa). End bp sat process by clicking "proceed to the next step" (consolidation).

Positioning cameras and lights

This must be completed during back pressure saturation, before consolidation begins! Cameras are connected to the Image computer. A signal from "Biax" computer (computer controlling test DAQ) controls taking pictures automatically through the Labview code. Images are stored in "Image" computer (adjacent computer). ***A USB key is needed for VIC Snap to run!***

1. Set the camera(s) and connect the wire(s) to Image computer and camera(s):
    a. Connect camera trigger cable (brown cable from DAQ box) to black adaptor wire. Screw in adaptor/trigger to bottom circular port on back of camera.

b. Connect one end of "I394" cable (marked "2" and "CPU") to either I394 port on the BACK bottom of the "image" computer. Connect other end (marked "camera") to either port on the upper back part of the camera (we've been using the left side)

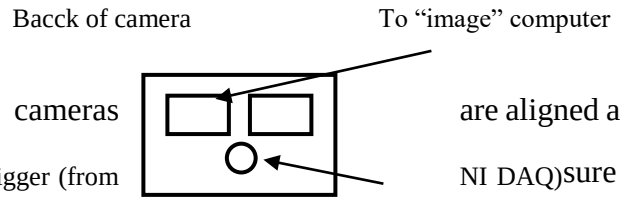

2. Make sure the cameras are aligned and centered with the specimen. Make sure the cameras are level and not tilted forward, back, or to the side! The lens face should be parallel to the specimen face and should be on the same level as the specimen's center. Aim to have the camera as close as possible to the specimen.
3. Set the lights, positioning to avoid reflections. Cover bright areas with something black.
4. Run the camera software, VICSnap, on Image computer (must have a USB Key!).
5. Create a folder on the desktop in which to store the test images.
6. The camera software should detect the cameras. Select a filename prefix (same as test name) and directory in which to store the image files (the folder you just created), and click OK.
7. Set up fans: pink fan next to biax computer (pull out drawer and set in drawer), aimed to right in front of camera; clamp-on fan on tripod on middle lab table; stainless fan on corner of lab table. Make sure fans do not cause light filters to flicker too much.
8. Focus each camera using the writing on the glass wall.
9. Move and rearrange lighting to get best lighting results. . It is worthwhile to spend some time making sure the images and lighting is as uniform as possible.
10. Try to have the aperture as open as possible. This will reduce the chance of having the focal length on the external glass in which case reflections and scratches will be an issue.
11. The room lights should be completely off when focusing cameras and collecting images.
12. Take two initial images of specimen: click "Capture".
13. If needed, compare images to images from a previous "good" test to assess brightness and contrast. If needed, adjust light positions and/or camera positions.
14. Continue adjustments until camera settings and lighting are satisfactory. Then, delete these images (or move to a different location), and restart VICSnap. The aim of this step is to zero the picture numbers, so that Labview (which numbers the pictures starting from zero) and VICSnap are synchronized.

15. Press on edit project and then change the folder to collect the images in a different folder and select names for images. The aim of this step is to zero the picture numbers. Make image numbers in VIC snap starting from zero. Labview code starts numbering from zero, so having image numbers in Labview synchronized with the image numbers in VICsnap helps identify images. Or, quit VC snap, move or delete all previous images and restart VIC.
16. In VIC-Snap, Under "images", select "Sync Mode", and then choose "Hardware". Go back to "Images" and select "Streaming Capture". Choose "Save 1 of every 1". Click "Start". Popup window will remain. Image will be saved everytime Labview sends a trigger. Window MAY be distorted at first and frozen. Ignore this, it will correct itself once the images begin capture.
17. The cameras are now ready.

Consolidation

1. Record burette water levels. Make sure valve 8 is closed and valve 7 opened.
2. Input the desired final effective confining stress, Kc = σ_3'/σ_1', and a data recording interval (in sec). Once started, an initial image and sensor data reading will be taken, and the loader will begin spinning at a given velocity. Cell pressure will only begin incrementing when the axial load has increased to a provide a vertical effective stress = $K_c \cdot \sigma_3'$. Then, cell pressure will increase in proportion to axial stress increases to maintain the specified K_c.
3. Once the desired cell pressure (effective pressure) is reached, the loader will stop, and the green button at the bottom right will turn bright green to say "Consolidation Complete". If for some reason a higher load is desired, click on "restart motor" and the motor will begin spinning again, and cell pressure will increase again according to K_c. When ready to proceed to shear, click "Proceed to Next Step".
4. Close burette valve 7. Then, open valve 8 in preparation for shear.

Shear and stopping test

1. Record burette water levels.
2. Close valve 7 (both burette valves are now closed). Then, open valve 8.
3. When prompted, specify the axial strain rate (% per hour), the data acquisition interval (in seconds), and the number of data points between images (integer number). Click to begin shear.

a. Note that the maximum velocity of the loader is 75. The equation for motor velocity is:

$$\frac{\text{Specimen Height} * \text{Desired Shear Rate}}{17.775}$$

Check if your specified strain rate is less than or equal to this velocity. Otherwise the axial loader will not run.

4. Run shear as long as possible. Shear is usually stopped when:
    a. one of the side or sled LVDTs become compressed all the way
    b. the membrane becomes overly stretched due to shear band offset (wrinkles in the membrane are evident); or some other obstruction occurs.
5. When you are sure shear is to be finished, click "Proceed to next step"
6. ***Close valve 2 and valve 3 (to avoid dirty water coming back into the burrettes)*** 7. Reduce back pressure to zero. Turn to valve 11 "vent". Press OK on Labview screen.
8. ***Close air release valve at top of apparatus***.
9. Press DONE on screen. Press stop and de-engerize motor. Press "Stop" in lower right corner to end Biax 3.0 v.1.
10. Disconnect air line from valve line coming from top of cell. Valve should remain closed and attached to top of cell.
11. Slowly reduce the pressure in the cell by slowly opening the valve. Noise may be loud.
12. Quit VIC-Snap.

Ending test and emptying cell from oil:

1. Have lots of paper towels handy!!!
2. Close burette main valve (Valve 10).
3. Disconnect top and bottom of specimen water lines from the base of biaxial, close the biaxial outlets with end caps.
4. If you did not have Labview reduce the cell pressure, then cell pressure must be reduced: The cell pressure should be whatever the consolidation pressure was. Close air valve at top of the cell, reduce compressed air to zero, disconnect air valve from the compressed air source tube, then slowly open the air valve (noise will be loud) to release the pressure. *Reconnect the tubing to the valve!*

5. Place one open end of the oil drainage line into a silicone container.
6. Open oil valve on the control panel (Valve 4) and open air release valve at top of tank. Oil should start flowing out of the cell to the oil tank by gravity. Slowly increase the cell pressure to 100 kPa to speed up the process. Be careful with using higher pressures. If the pressure is high, then the cell plate rod will slowly rise up.
7. When one of the silicone containers is near full:
    a. Close valve 4 and oil valve at bottom of biaxial device.
    b. Place open end of drainage line into another nearly empty silicone container.
    c. Open valve and oil valve at bottom of biaxial device.
8. When the cell is near empty, close Valve 4, the front bottom of cell and the air release valve at front top of cell and also oil valve. *Do not try to blow <u>all</u> the oil into the silicone oil containers. This will cause the silicone air in the cell to bubble.*
9. Remove oil drainage line from silicone container and close with a cap.
10. Reduce compressed air to zero. Close air valve leading to top of cell, disconnect the air tubing from valve, and open valve slowly (noise will be loud). This will reduce pressure in the cell to zero.
11. Remove air pressure hose from the front top of biaxial top plate.
12. Close main air pressure valve, Valve 1, on board.
13. Turn Motor controller off.
14. Close the oil valve line coming from front bottom of cell and remove (quick connect).
15. Open oil drainage caps in biaxial base. Let excess oil drain into a bowl. If possible. Have someone help you tip the biaxial device to let as much oil drain out.

Disassembling Cell and Specimen:

1. Tighten axial rod in the top plate. (External axial rod collar).
2. Remove axial rod guide pin from base of axial loader motor.
3. Loosen axial rod-motor connection from both sides. Rotate screw rod all the way up.
4. Loosen two nuts that fasten motor to top platen.
5. Remove loader and place on shelf. Tighten in place.
6. Loosen the 4 nuts on top plate. Store properly along with the 4 rubber washers.

7. Unscrew axial rod connector (hold rod tightly). Raise axial rod all the way up. Retighten. 8. Lift top plate uniformly with a big screwdriver and remove. Store properly 9. Unscrew and remove the 4 tall rods around the cell. Store properly.
10. Using big screw driver, carefully lift Plexiglas cell off the base O-ring. Carefully remove cell without scratching the inside. Store on paper towels on dolly.
11. Wipe off oil residue off cell with Kimwipes. Cover cell during storage.
12. Place MANY paper towels around biaxial base on table to catch dripping oil.
13. Untie the sensor wires.
14. Remove LVDTs from holders. Place neatly and safely on towels on biaxial table.
15. Remove LVDT holders, wipe off excess oil and place on towels on biaxial table.
16. Unscrew the screws on the load cell (if needed raise black bar to have more room to unscrew the screws.)
17. ***Hold the specimen securely!*** Lower black cross bar, tighten collar, raise cross bar all the way. Now the specimen is unsupported and may fall, so hold tightly!
18. Disconnect the drainage lines from the platens. Place them outside the cell base so they do not become contaminated with oil. *Continue to hold specimen securely*!
19. Loosen and remove sidewall tie rods. Place on paper towels.
20. Remove the specimen from the sled. Remove the top O-rings and top platen and put by sink for cleaning. *Wipe off as much excess grease from the platen and o-rings as possible!* Remove the filter papers and platen membranes and throw away.
21. Remove material from specimen membrane: material near the platens is covered with grease and must be discarded, but the material near the center of the specimen can be dried and reused. When removing the "good" material from the specimen, use care not to get grease/oil into the material.
22. Loosen sidewall screws connected to the sled.
23. Cautiously lift load cell glass wall and place next to the biaxial device.
24. Unscrew glass/plexiglass connectors and separate walls, remove load cells and place them on paper towels under biaxial device.
25. Place load cells on paper towels on biaxial table and wipe off any oil.
26. Wipe excess oil off of glass walls with Kimwipes. Place next to sink on paper towels to be cleaned.

27. Cautiously remove second sidewall.
28. Remove screws on side of glass, separate walls.
29. Slide glass apart, wipe off excess oil with Kimwipes, and place the walls next to the sink on paper towels to be cleaned.
30. Carefully remove the specimen and platens. Wipe off ALL excess grease and oil with Kimwipes.
31. Empty sand into a porcelain dish. Place sand in oven to dry. Remove bottom platen and Orings. Wipe excess grease/oil off of platens with Kimwipes. Wipe excess oil off of O-rings with paper towels.
32. Thoroughly wash with soap and water (gently, with a sponge) the platens and sidewalls. Then, dry, and clean with Windex.
33. Remove porous stones from platens and boil in demineralized water for 10 minutes. Every 3^{rd} to 4^{th} test, soak porous stones in vinegar for four hours, then reboil and dry.
34. Wipe off oil residues from the inner frame and all other parts in the biaxial base. Make sure all sand is removed from bottom sled.
35. Place all tools in their respective places.

Appendix

The main tools used to assemble the apparatus are:

Allen wrenches: 1/4, 3/16, 5/32, 9/64

Regular wrenches: ½ – 9/16, ½ –7/16, 7/16, 9/16, adjustable wrench

Scissors

Screw drivers

Picture 1 Screw drivers and wrenches

Dow corning vacuum grease is used to lubricate the top and bottom platens if desired. Grease is also used to fill the grooves where the orings sit in order to secure tight seal.

Picture 2 Dow corning vacuum grease

The main tools used to prepare the specimen are:

- Spoon
- Brushes
- Scraper

Picture 3 Specimen preparation tools

One of the two glass walls through which pictures are taken. Glass walls should be cleaned using Kimwipes only. Tick marks in the glass wall should be marked and a test number should be written on the sample side of the glass wall (will help focus the camera and establish image scale). Black color is not very good because the background of the pictures is black which makes it very hard to read

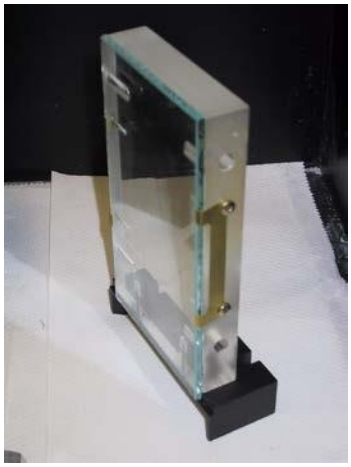

Picture 4 Glass wall

This is the burette system. Burettes are filled with de-aired de-mineralized water only. There are two small burettes that are seldom used because of the capillary action. The two big burettes hold about 80 cc of water. A differential pressure transducer (DP) attached to the left of the burettes electronically measure the change in water volume by relating change in volume to change in pressure head. Burettes can be controlled individually or in groups. For example the two big burettes can be used together, two small together or each burette can be used separately.

Picture 5 Burettes

The motor is used to apply axial load and or displacement to the top of the specimen. The small part in the top of the picture is the actual motor. The black metal frame contains a reducer with high reduction ratio. The motor has been calibrated so certain volts correspond to certain rotation per minute that is in turn correlated to mm/minute linear velocity. The motor system is used to apply constant velocity to shear the specimen. The Labview code is smartly built to control the motor and enables stress controlled testing where the motor shaft advances while maintaining a constant applied force measured by a load cell.

Picture 6 Motor

Close up picture for the motor shaft. The shaft position can be manually changed by loosening the aligning rod and twisting the screw. At the beginning of every test the shaft should be positioned in such a way that no initial displacement is applied to the specimen when the motor is mounted onto the axial rod. The black connector connects the motor shaft to the axial rod through the top platen. Four screws need to be tightened well to make sure the axial rod does not slip.

Picture 7 Motor shaft

When running CO_2 through the specimen, the top drainage is connected to a hose with its end in a water beaker. This helps monitor the flow of CO_2. CO_2 is applied from the bottom of the specimen at approximately 2.5 psi or 15 kPa. The specimen has to be confined with cell pressure higher than the CO_2 pressure prior to the application of CO_2. It is enough to flush the specimen with CO_2 for 3o minutes.

Picture 8 CO_2 hose in water beaker

After placing a uniform grease layer on the glass surface, a cut triaxial membrane is placed on the grease to separate grease from sand. The membrane has an opening in the middle a little bigger that the porous stone. The porous stone should not be covered by the membrane otherwise water drainage will be clogged. It is a good practice to make sure no air bubbles are underneath the membrane. In the picture you see the bottom platen.

Picture 9 Making sure triaxial membrane doesn't have air bubbles underneath

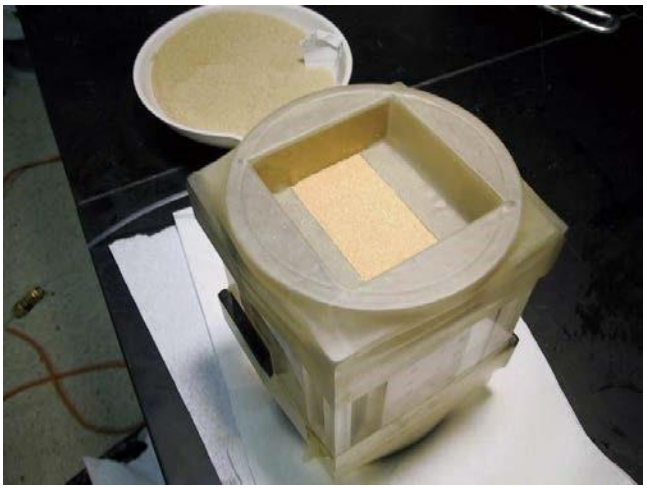

After filling the mold with sand, loose or dense, it is necessary to make the surface flush with the mold. The process of leveling the surface is very delicate and time consuming. It is very important that minimal disturbances get applied to the specimen. Experience shows that be performing this step right the likelihood of the shear band hitting the platens decreases significantly

Picture 10 Sand flush with mold

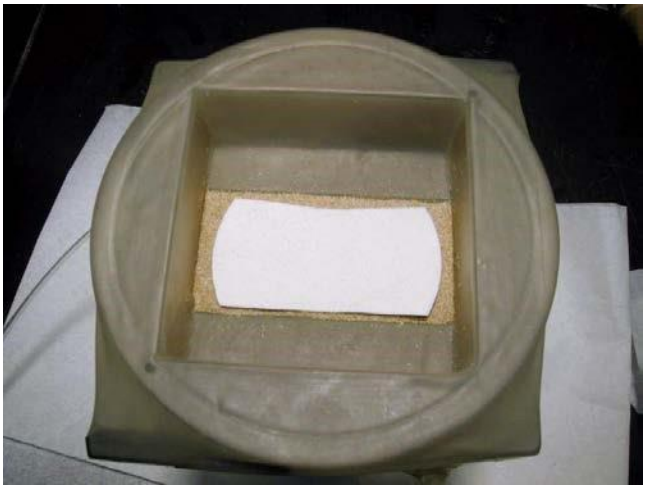

Placing a filter paper at the bottom and top of the specimen is crucial. The filter paper should be centered on the porous stone. **NOTE: filter paper should be cut a little smaller than shown here**!

Picture 11 Placing filter paper on top of specimen

This picture shows the top platen axial rod in its upper most position. The axial rod should be in this position before placing the top platen. After placing the top platen, the axial rod break should be released and the rod slowly advanced as close as possible but not touching the screw (in the middle of picture) attached to the internal axial rod. The top platen axial rod break should be tightened again after rod is in position. This ensures that no initial shearing displacement is applied to the specimen when the motor is placed in position.

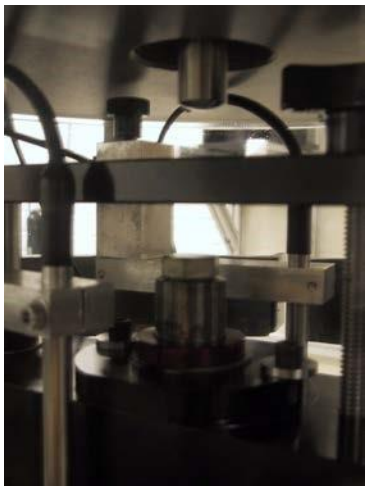

Picture 12 Top platen rod and internal axial rods

Appendix B Sample Calculations

Reduced Data from Biaxial Tests

GLOBAL DATA

Test Identification: test_id := "S-2"

Soil type: Soil_Type := "Ottawa 20-30 Sand"

Loading rate: load_rate := 0.9 %/hr

Membrane thickness: $t_m := 0.39mm$

Units: kPa := 10^3Pa kN := 10^3N

SAMPLE PREPARATION DATA

Water Content (click to expand)

Density

Sample height: $h := 139.7 \cdot mm = 139.70 \cdot mm$

Sample width:	$w_0 := 82.31mm$	$w_1 := 82.29mm$	$w_2 := 82.18mm$
Sample thickness:	$t_0 := 41.44mm$	$t_1 := 42.11mm$	$t_2 := 42.44mm$
Total mass:	$m_i := 1647.36gm$	$m_f := 909.39gm$	$m_t := m_i - m_f$
Specific gravity of soil solids:		$G_s := 2.67$	
Density of water:		$\rho_w := 0.99707 \frac{gm}{cm^3}$	
Maximum and minimum void ratios:		$e_{max} := 0.742$	$e_{min} := 0.502$
Sample dimensions:		$h_s := h + 2 \cdot t_m$	$h_s = 140.480 \cdot mm$
		$w_s := mean(w) - 2 \cdot t_m$	$w_s = 81.480 \cdot mm$
		$t_s := mean(t) - 2 \cdot t_m$	$t_s = 41.217 \cdot mm$
Sample volume:	$V_{sam} := h_s \cdot w_s \cdot t_s$	$V_{sam} = 4.718 \times 10^5 \cdot mm^3$	
Density of soil solids:	$\rho_s := G_s \cdot \rho_w$	$\rho_s = 2.662 \cdot \frac{gm}{cm^3}$	
Mass of soil:	$m_t = 737.970 \cdot gm$	$m_s := (1 - w_g) \cdot m_t$	$m_s = 737.970 \cdot gm$

Sample dry density: $\rho_d := \frac{m_s}{V_{sam}}$ $\rho_d = 1.564 \cdot \frac{gm}{cm^3}$

Sample void ratio: $e := \frac{\rho_s}{\rho_d} - 1$ $e = 0.702$

Sample relative density: $D_r := \frac{e_{max} - e}{e_{max} - e_{min}}$ $D_r = 16.704 \cdot \%$

INPUT DATA

Note that the data from the Agilent 34770A DMM is output as comma-separated values with three columns each for the fourteen measured channels. Columns for each channel are (in order) time stamp, time (seconds), and reading (VDC).

Filename containing raw data: data :=

S-2 SH.xlsx

Number of channels measured: nchan := 15

Remove the last row of the data matrix as it most likely contains some zero measurements:

data := submatrix(data, 0, rows(data) − 2, 0, cols(data) − 1)

Use visual inspection to determine the number of rows of data to be omitted from the beginning of the test to compensate for seating time.

Number of rows to remove: rem_rows := 3 end_rows := rows(data) − 1

data := submatrix(data, rem_rows, end_rows, 0, cols(data) − 1)

Number of columns (channels x 3): ncols := cols(data) ncols = 21.000

Number of rows (data points): nrows := rows(data) nrows = 4.547×10^3

Extract the columns containing time data from the main matrix:

i := 0 .. nchan − 1 time := $data^{\langle 0 \rangle} \cdot s$

Subtract baseline readings to normalize data:

baseline := $(data^T)^{\langle 0 \rangle}$ $data^{\langle i \rangle} := data^{\langle i \rangle} - baseline_i$

BUOYANT WEIGHT DATA AND CALCULATIONS (click to expand)

CALIBRATION FACTORS FOR EACH CHANNEL (click to expand)

CALCULATE LOAD AND DISPLACEMENT

$$disp := [(submatrix(data, 0, nrows - 1, 8, 14)) \cdot mm]$$

$$force := submatrix(data, 0, nrows - 1, 1, 7) \cdot kg \cdot g$$

CALCULATION OF GLOBAL STRESS AND STRAIN (based on Drescher, et al., 1990)

Indices: $n := 0 .. nrows - 1$

Confining Stress: $\sigma_{3_n} := 10 \cdot psi$

Sample thickness (upper): $t_u := t_s - \left[(disp)^{\langle 2 \rangle} + disp^{\langle 4 \rangle}\right]$

Sample thickness (lower): $t_l := t_s - \left(disp^{\langle 3 \rangle} + disp^{\langle 5 \rangle}\right)$

Sample thickness (average): $d_{2_n} := mean\left(t_{u_n}, t_{l_n}\right)$

Average thickness minus the sled displacement

$$d_{2a_n} := mean\left(t_{u_n}, t_{l_n}\right) - \left(disp^{\langle 6 \rangle}\right)_n$$

Sample axial deformation: $u_{a_n} := mean\left[\left[-\left(disp^{\langle 1 \rangle}\right)\right]_n\right]$ Only one axial LVDT working

Sample height: $d_{1_n} := h_s - u_a$

Natural strains: $\varepsilon_1 := -\ln\left(1 - \frac{u_a}{h_s}\right)$ $\varepsilon_2 := -\ln\left(\frac{d_2}{t_s}\right)$ $\varepsilon_{2a} := -\ln\left(\frac{d_{2a}}{t_s}\right)$

Volumetric and shear strains: $\varepsilon_v := \varepsilon_1 + \varepsilon_2$ $\gamma := \varepsilon_1 - \varepsilon_2$ $\varepsilon_{va} := \varepsilon_1 + \varepsilon_{2a}$

Calculation of average axial load (see *drescher data reduction.mcd*):

Area of loading piston: $d_p := \begin{pmatrix} 25.40 \\ 25.38 \\ 25.37 \end{pmatrix} mm$ $A_p := \frac{1}{4}\pi \cdot mean\left(d_p\right)^2$

Initial loads:

$P_{10} := \sigma_3 \cdot A_p$ Axial

$P_{20} := \left(force^{\langle 1 \rangle}\right)_0$ Bottom Right Center

$P_{30} := \left(force^{\langle 2 \rangle}\right)_0$ Bottom Left Front

$P_{40} := \left(force^{\langle 3 \rangle}\right)_0$ Bottom Left Back

$P_{50} := \left(force^{\langle 4 \rangle}\right)_0$ Side Top

$P_{60} := \left(force^{\langle 5 \rangle}\right)_0$ Side Middle

$P_{70} := \left(force^{\langle 6 \rangle}\right)_0$ Side Bottom

Load on base platen: $P_L := force^{\langle 1 \rangle} + force^{\langle 2 \rangle} + force^{\langle 3 \rangle} - P_{20} - P_{30} - P_{40}$

Load on upper platen: $P_u := force^{\langle 0 \rangle} - P_{10}$

Load on side wall: $P_s := \left(force^{\langle 4 \rangle} + force^{\langle 5 \rangle}\right) - P_{50} - P_{60}$

Average axial load: $P := P_L + \frac{\left(P_u - P_L + W_{top} - 2 \cdot W_{bot} - \frac{W_{sam}}{2}\right)}{3}$

Major principal stress: $\sigma_1 := \overrightarrow{\left(\frac{P}{w_s \cdot d_2}\right)} + \sigma_3$

Intermediate principal stress: $\sigma_2 := \sigma_3 + \frac{\overrightarrow{P_s}}{d_1 \cdot d_2}$

Stress at base platen: $\sigma_b := \sigma_3 + \frac{\overrightarrow{P_L}}{w_s \cdot d_2}$

System friction: $f1_n := \left|\frac{Pu_n - PL_n}{P_n}\right|$ Method 1 $f2_n := \left|\frac{Pu_n - PL_n}{mean\left(Pu_n, PL_n\right)}\right|$ Method 2 $f_n := \frac{f1_n - f2_n}{mean\left(f1_n, f2_n\right)}$ Difference

Mobilized friction angle: $\phi_m := asin\left(\frac{\overrightarrow{\sigma_1 - \sigma_3}}{\sigma_1 + \sigma_3}\right)$

Calculation and output file:

$\varepsilon_{ax} := \frac{u_a}{h_s}$ $output := augment\left(\frac{\sigma_1}{Pa}, \frac{\sigma_3}{Pa}, \varepsilon_{ax}, \varepsilon_v\right)$ $WRITEPRN(concat(test\_id, ".out")) := output$

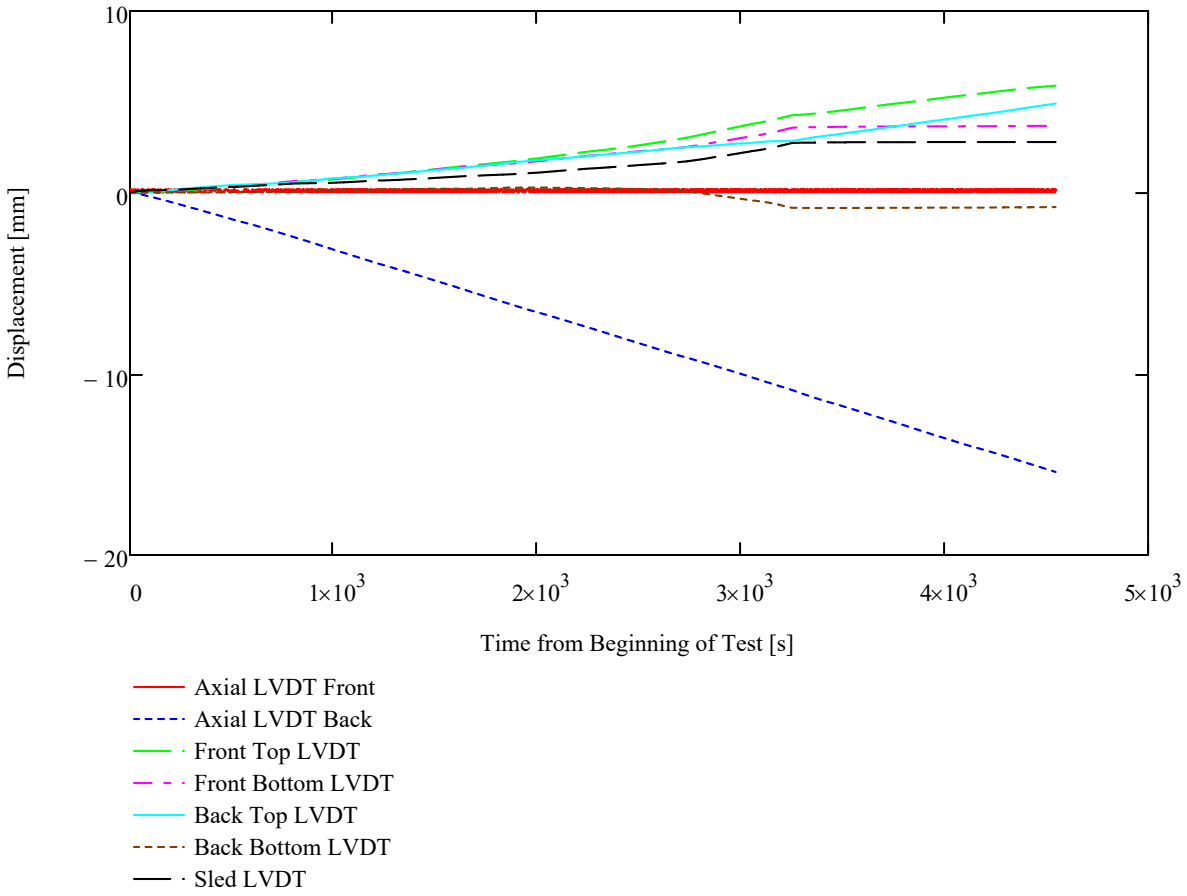
10
0
– 10
– 20
Displacement [mm]
0
1×10^3
2×10^3
3×10^3
4×10^3
5×10^3
Time from Beginning of Test [s]
Axial LVDT Front
Axial LVDT Back
Front Top LVDT
Front Bottom LVDT
Back Top LVDT
Back Bottom LVDT
Sled LVDT

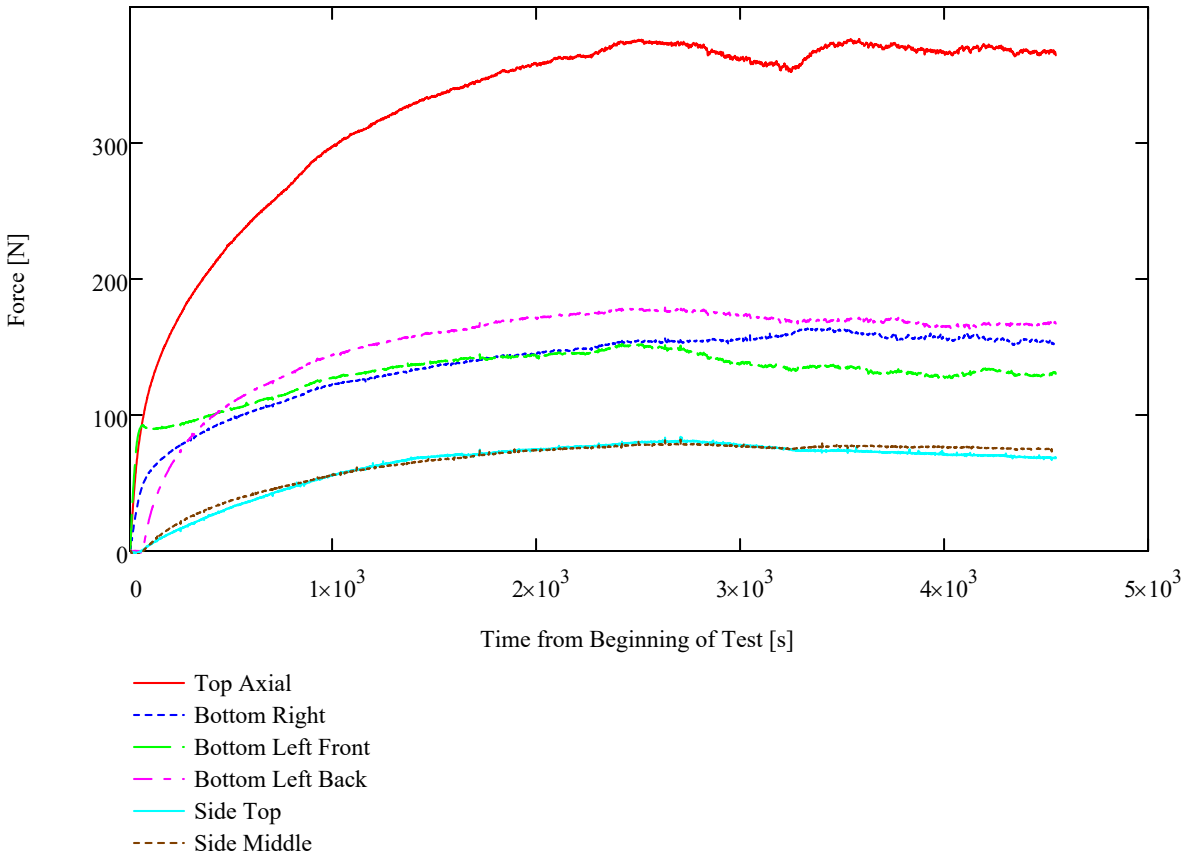
Force [N]
300
200
100
0
0
1×10^3
2×10^3
3×10^3
4×10^3
5×10^3
Time from Beginning of Test [s]
Top Axial
Bottom Right
Bottom Left Front
Bottom Left Back
Side Top
Side Middle

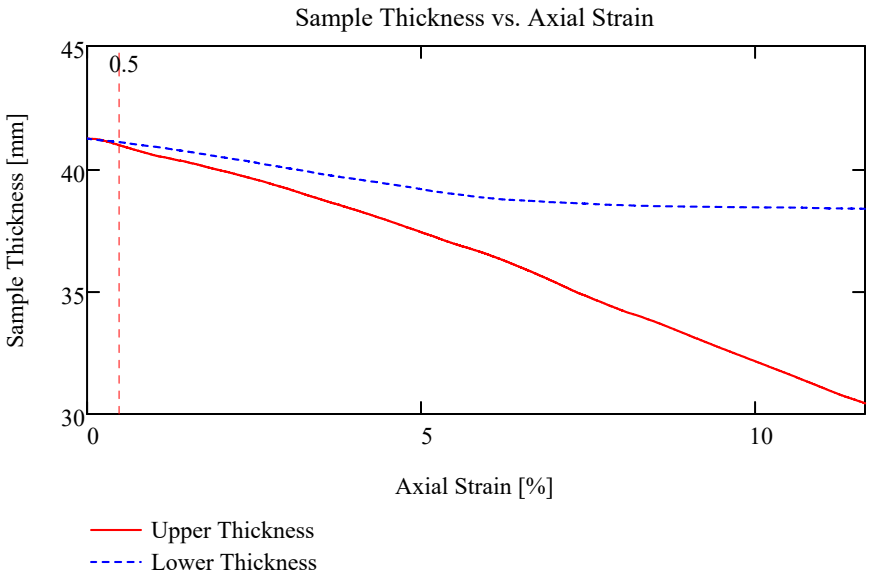
Sample Thickness vs. Axial Strain
Sample Thickness [mm]
45
40
35
30
0.5
0
5
10
Axial Strain [%]
Upper Thickness
Lower Thickness

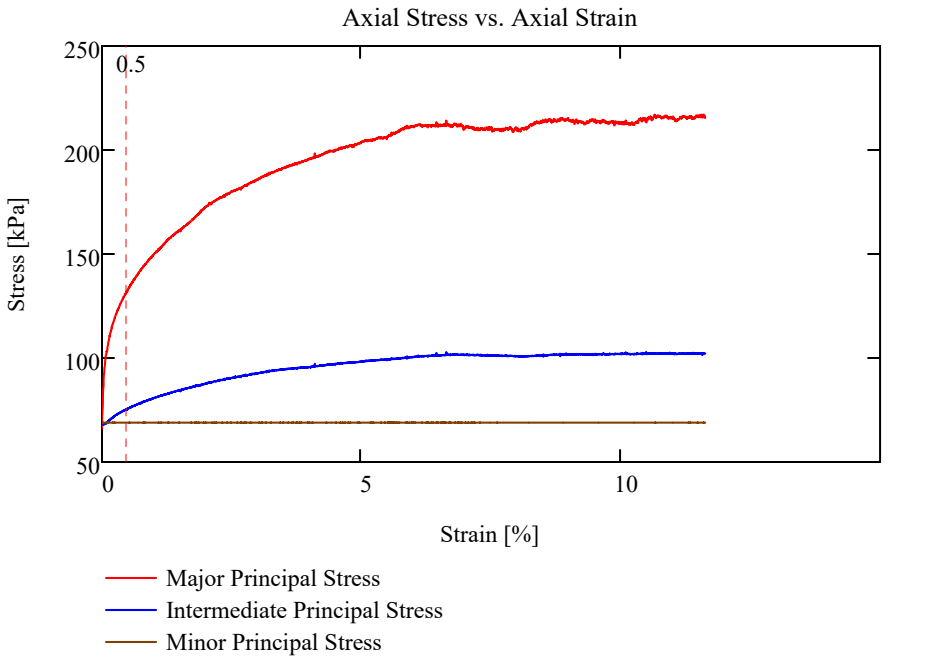
Axial Stress vs. Axial Strain
250
200
150
100
50
0.5
Stress [kPa]
0
5
10
Strain [%]
Major Principal Stress
Intermediate Principal Stress
Minor Principal Stress

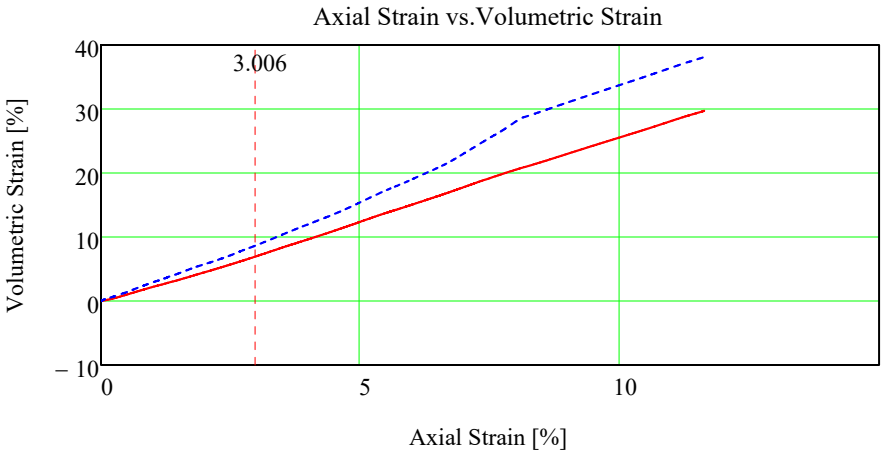
Axial Strain vs.Volumetric Strain
40
30
20
10
0
– 10
3.006
Volumetric Strain [%]
0
5
10
Axial Strain [%]

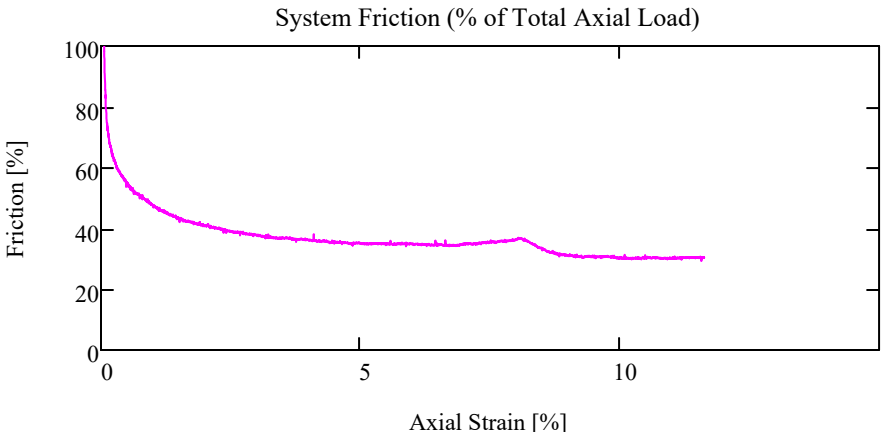

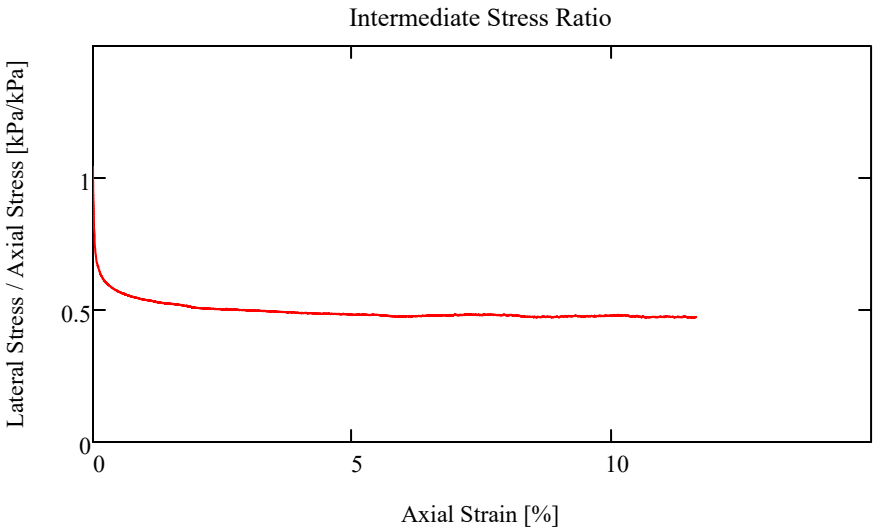

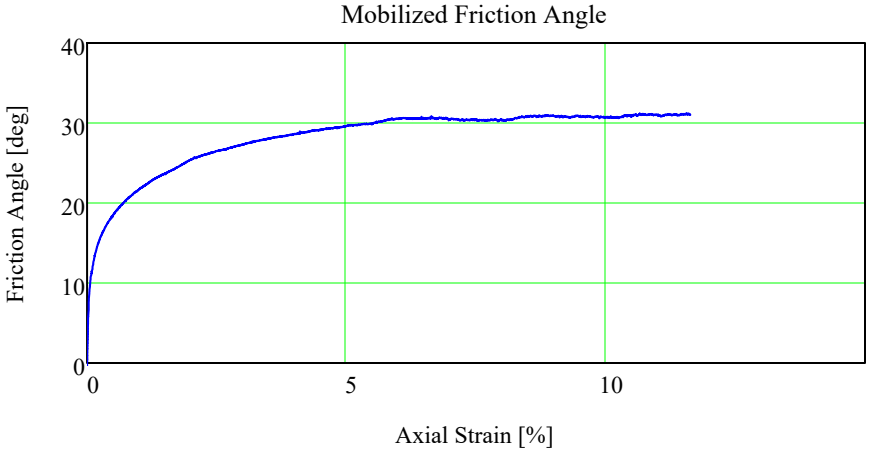

CALCULATION OF STRESS AND STRAIN AFTER THE ONSET OF LOCALIZATION

(based on Drescher, et al., 1990)

Inclination of failure plane: $\theta_e := 50deg$

Global strain at onset of shear banding: $\varepsilon_b := 0.5\%$

Shift data vectors to correspond to the onset of shear banding:

$$\text{Locate}(v,\varepsilon) := \begin{| i \leftarrow 0 \\ L \leftarrow 0 \\ \text{for } m \in 0..\text{last}(v) \\ \quad \text{if } v_m \geq \varepsilon \\ \quad\quad L \leftarrow m \\ \quad\quad \text{return } L \end{|}$$

$\text{new} := \text{Locate}(\varepsilon_1, \varepsilon_b)$

$\text{new} = 254$

$u_h := \text{disp}^{\langle 6 \rangle}$ $\quad p := \text{new}..\text{nrows} - 1$

$u_{hh_{p-new}} := u_{h_p}$ $\quad u_{aa_{p-new}} := u_{a_p}$ $\quad \sigma_{11_{p-new}} := \sigma_{1_p}$ $\quad \sigma_{33_{p-new}} := \sigma_{3_p}$

$t_{h_{p-new}} := \text{time}_p - \text{time}_{new}$ $\quad \varepsilon_{1h_{p-new}} := \varepsilon_{1_p} - \varepsilon_{1_{new}}$

Calculate incremental axial and sled displacements:

$i := 0..\text{last}(u_{hh}) - 1$ $\quad \Delta u_{h_i} := u_{hh_{i+1}} - u_{hh_i}$ $\quad \Delta u_{a_i} := u_{aa_{i+1}} - u_{aa_i}$

Normal stress on failure plane: $\sigma_n := \sigma_{11} \cdot \cos(\theta_e)^2 + \sigma_{33} \cdot \sin(\theta_e)^2$

Shear stress on failure plane: $\sigma_s := (\sigma_{11} - \sigma_{33}) \cdot \cos(\theta_e) \cdot \sin(\theta_e)$

Friction on the shear band: $\phi_s := \text{atan}\left(\frac{\overrightarrow{\sigma_s}}{\sigma_n}\right)$

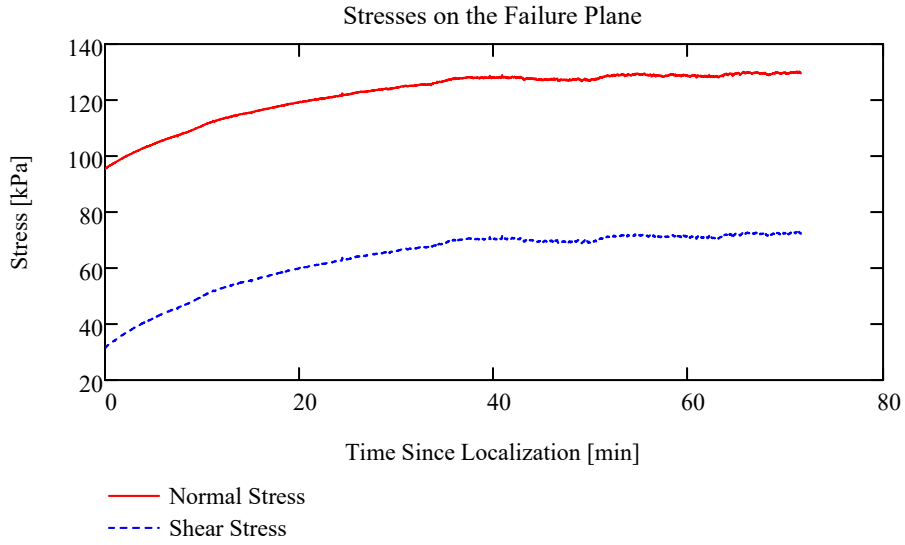
Stresses on the Failure Plane
Stress [kPa]
140
120
100
80
60
40
20
0
20
40
60
80
Time Since Localization [min]
Normal Stress
Shear Stress

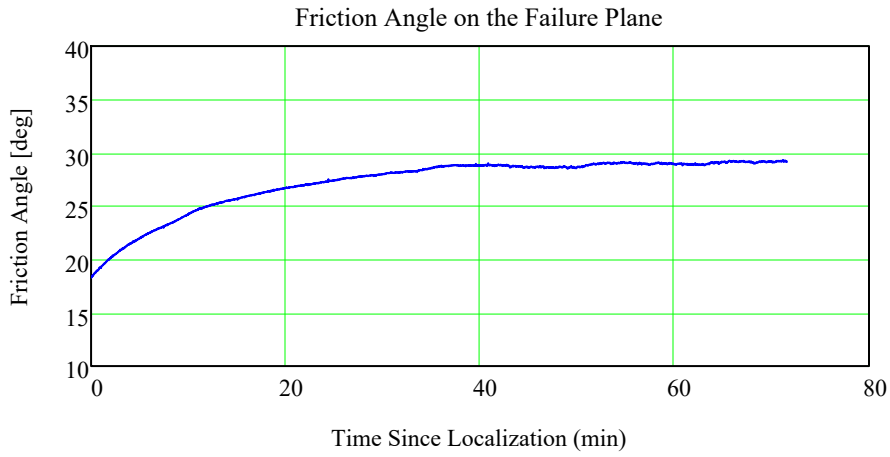
Friction Angle on the Failure Plane
Friction Angle [deg]
40
35
30
25
20
15
10
0
20
40
60
80
Time Since Localization (min)

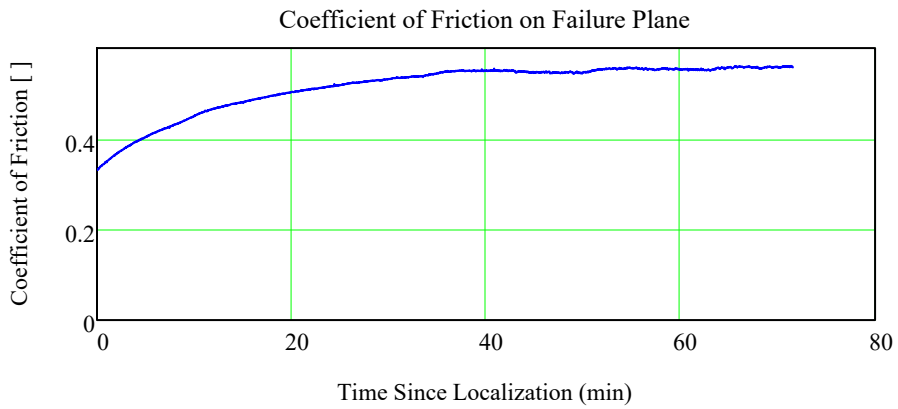
Coefficient of Friction on Failure Plane
Coefficient of Friction [ ]
0.4
0.2
0
0
20
40
60
80
Time Since Localization (min)

Reduced Data from Biaxial Tests

GLOBAL DATA

Test Identification: test_id := "S-2"

Soil type: Soil_Type := "Ottawa 20-30 Sand"

Loading rate: load_rate := 0.9 %/hr

Membrane thickness: $t_m := 0.39mm$

Units: kPa := 10^3Pa kN := 10^3N

SAMPLE PREPARATION DATA

Water Content (click to expand)

Density

Sample height: $h := 139.7 \cdot mm = 139.70 \cdot mm$

Sample width:	$w_0 := 82.31mm$	$w_1 := 82.29mm$	$w_2 := 82.18mm$
Sample thickness:	$t_0 := 41.44mm$	$t_1 := 42.11mm$	$t_2 := 42.44mm$
Total mass:	$m_i := 1647.36gm$	$m_f := 909.39gm$	$m_t := m_i - m_f$
Specific gravity of soil solids:		$G_s := 2.67$	
Density of water:		$\rho_w := 0.99707 \frac{gm}{cm^3}$	
Maximum and minimum void ratios:		$e_{max} := 0.742$	$e_{min} := 0.502$
Sample dimensions:		$h_s := h + 2 \cdot t_m$	$h_s = 140.480 \cdot mm$
		$w_s := mean(w) - 2 \cdot t_m$	$w_s = 81.480 \cdot mm$
		$t_s := mean(t) - 2 \cdot t_m$	$t_s = 41.217 \cdot mm$
Sample volume:	$V_{sam} := h_s \cdot w_s \cdot t_s$	$V_{sam} = 4.718 \times 10^5 \cdot mm^3$	
Density of soil solids:	$\rho_s := G_s \cdot \rho_w$	$\rho_s = 2.662 \cdot \frac{gm}{cm^3}$	
Mass of soil:	$m_t = 737.970 \cdot gm$	$m_s := (1 - w_g) \cdot m_t$	$m_s = 737.970 \cdot gm$

Sample dry density: $\rho_d := \frac{m_s}{V_{sam}}$ $\rho_d = 1.564 \cdot \frac{gm}{cm^3}$

Sample void ratio: $e := \frac{\rho_s}{\rho_d} - 1$ $e = 0.702$

Sample relative density: $D_r := \frac{e_{max} - e}{e_{max} - e_{min}}$ $D_r = 16.704 \cdot \%$

INPUT DATA

Note that the data from the Agilent 34770A DMM is output as comma-separated values with three columns each for the fourteen measured channels. Columns for each channel are (in order) time stamp, time (seconds), and reading (VDC).

Filename containing raw data: data :=

S-2 SH.xlsx

Number of channels measured: nchan := 15

Remove the last row of the data matrix as it most likely contains some zero measurements:

data := submatrix(data, 0, rows(data) − 2, 0, cols(data) − 1)

Use visual inspection to determine the number of rows of data to be omitted from the beginning of the test to compensate for seating time.

Number of rows to remove: rem_rows := 3 end_rows := rows(data) − 1

data := submatrix(data, rem_rows, end_rows, 0, cols(data) − 1)

Number of columns (channels x 3): ncols := cols(data) ncols = 21.000

Number of rows (data points): nrows := rows(data) nrows = 4.547×10^3

Extract the columns containing time data from the main matrix:

i := 0 .. nchan − 1 time := $data^{\langle 0 \rangle} \cdot s$

Subtract baseline readings to normalize data:

baseline := $(data^T)^{\langle 0 \rangle}$ $data^{\langle i \rangle} := data^{\langle i \rangle} - baseline_i$

BUOYANT WEIGHT DATA AND CALCULATIONS (click to expand)

CALIBRATION FACTORS FOR EACH CHANNEL (click to expand)

CALCULATE LOAD AND DISPLACEMENT

$$disp := [(submatrix(data, 0, nrows - 1, 8, 14)) \cdot mm]$$

$$force := submatrix(data, 0, nrows - 1, 1, 7) \cdot kg \cdot g$$

CALCULATION OF GLOBAL STRESS AND STRAIN (based on Drescher, et al., 1990)

Indices: $n := 0 .. nrows - 1$

Confining Stress: $\sigma_{3_n} := 10 \cdot psi$

Sample thickness (upper): $t_u := t_s - \left[(disp)^{\langle 2 \rangle} + disp^{\langle 4 \rangle}\right]$

Sample thickness (lower): $t_l := t_s - \left(disp^{\langle 3 \rangle} + disp^{\langle 5 \rangle}\right)$

Sample thickness (average): $d_{2_n} := mean\left(t_{u_n}, t_{l_n}\right)$

Average thickness minus the sled displacement

$$d_{2a_n} := mean\left(t_{u_n}, t_{l_n}\right) - \left(disp^{\langle 6 \rangle}\right)_n$$

Sample axial deformation: $u_{a_n} := mean\left[\left[-\left(disp^{\langle 1 \rangle}\right)\right]_n\right]$ Only one axial LVDT working

Sample height: $d_{1_n} := h_s - u_a$

Natural strains: $\varepsilon_1 := -\ln\left(1 - \frac{u_a}{h_s}\right)$ $\varepsilon_2 := -\ln\left(\frac{d_2}{t_s}\right)$ $\varepsilon_{2a} := -\ln\left(\frac{d_{2a}}{t_s}\right)$

Volumetric and shear strains: $\varepsilon_v := \varepsilon_1 + \varepsilon_2$ $\gamma := \varepsilon_1 - \varepsilon_2$ $\varepsilon_{va} := \varepsilon_1 + \varepsilon_{2a}$

Calculation of average axial load (see *drescher data reduction.mcd*):

Area of loading piston: $d_p := \begin{pmatrix} 25.40 \\ 25.38 \\ 25.37 \end{pmatrix} mm$ $A_p := \frac{1}{4}\pi \cdot mean\left(d_p\right)^2$

Initial loads:

$P_{10} := \sigma_3 \cdot A_p$ Axial

$P_{20} := \left(force^{\langle 1 \rangle}\right)_0$ Bottom Right Center

$P_{30} := \left(force^{\langle 2 \rangle}\right)_0$ Bottom Left Front

$P_{40} := \left(force^{\langle 3 \rangle}\right)_0$ Bottom Left Back

$P_{50} := \left(force^{\langle 4 \rangle}\right)_0$ Side Top

$P_{60} := \left(force^{\langle 5 \rangle}\right)_0$ Side Middle

$P_{70} := \left(force^{\langle 6 \rangle}\right)_0$ Side Bottom

Load on base platen: $P_L := force^{\langle 1 \rangle} + force^{\langle 2 \rangle} + force^{\langle 3 \rangle} - P_{20} - P_{30} - P_{40}$

Load on upper platen: $P_u := force^{\langle 0 \rangle} - P_{10}$

Load on side wall: $P_s := \left(force^{\langle 4 \rangle} + force^{\langle 5 \rangle}\right) - P_{50} - P_{60}$

Average axial load: $P := P_L + \frac{\left(P_u - P_L + W_{top} - 2 \cdot W_{bot} - \frac{W_{sam}}{2}\right)}{3}$

Major principal stress: $\sigma_1 := \overrightarrow{\left(\frac{P}{w_s \cdot d_2}\right)} + \sigma_3$

Intermediate principal stress: $\sigma_2 := \sigma_3 + \frac{\overrightarrow{P_s}}{d_1 \cdot d_2}$

Stress at base platen: $\sigma_b := \sigma_3 + \frac{\overrightarrow{P_L}}{w_s \cdot d_2}$

System friction: $f1_n := \left|\frac{Pu_n - PL_n}{P_n}\right|$ Method 1 $f2_n := \left|\frac{Pu_n - PL_n}{mean\left(Pu_n, PL_n\right)}\right|$ Method 2 $f_n := \frac{f1_n - f2_n}{mean\left(f1_n, f2_n\right)}$ Difference

Mobilized friction angle: $\phi_m := asin\left(\frac{\overrightarrow{\sigma_1 - \sigma_3}}{\sigma_1 + \sigma_3}\right)$

Calculation and output file:

$\varepsilon_{ax} := \frac{u_a}{h_s}$ $output := augment\left(\frac{\sigma_1}{Pa}, \frac{\sigma_3}{Pa}, \varepsilon_{ax}, \varepsilon_v\right)$ $WRITEPRN(concat(test\_id, ".out")) := output$

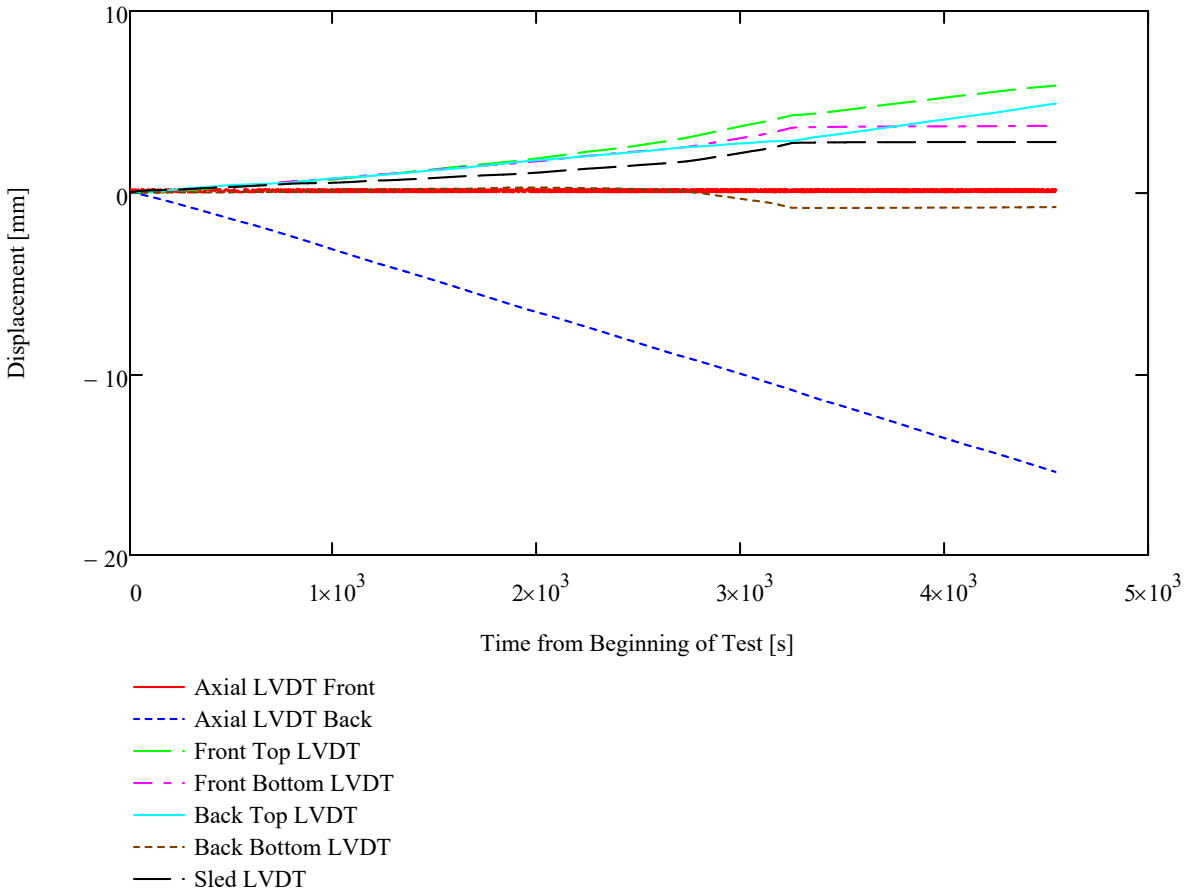
10
0
– 10
– 20
Displacement [mm]
0
1×10^3
2×10^3
3×10^3
4×10^3
5×10^3
Time from Beginning of Test [s]
Axial LVDT Front
Axial LVDT Back
Front Top LVDT
Front Bottom LVDT
Back Top LVDT
Back Bottom LVDT
Sled LVDT

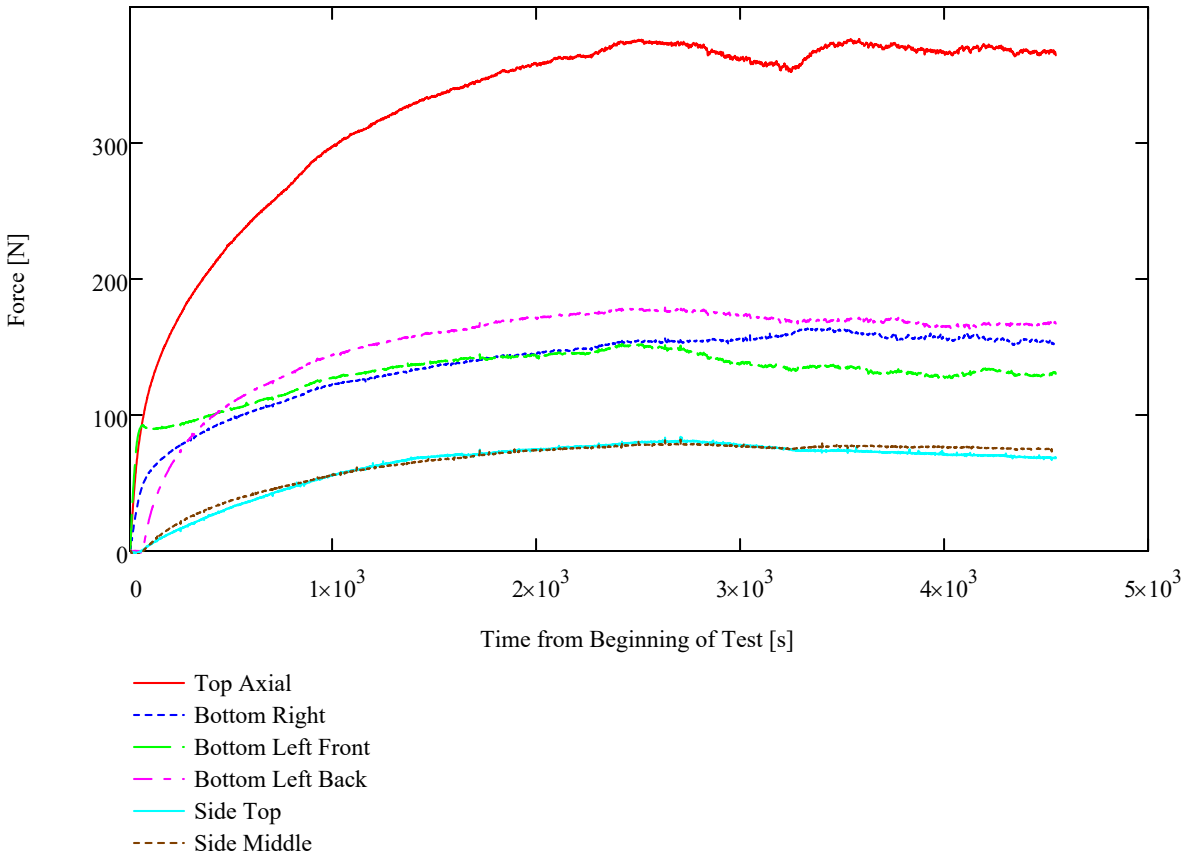
Force [N]
300
200
100
0
0
1×10^3
2×10^3
3×10^3
4×10^3
5×10^3
Time from Beginning of Test [s]
Top Axial
Bottom Right
Bottom Left Front
Bottom Left Back
Side Top
Side Middle

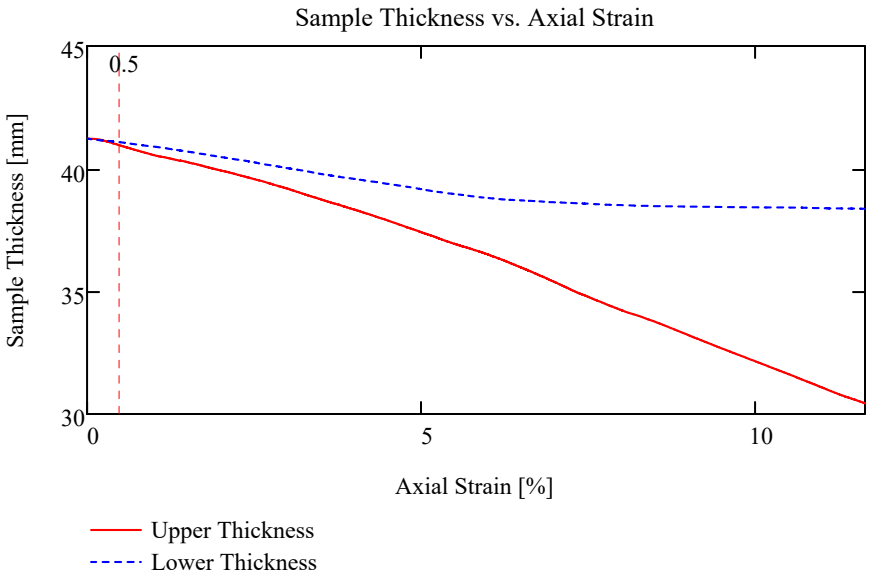
Sample Thickness vs. Axial Strain
Sample Thickness [mm]
45
40
35
30
0.5
0
5
10
Axial Strain [%]
Upper Thickness
Lower Thickness

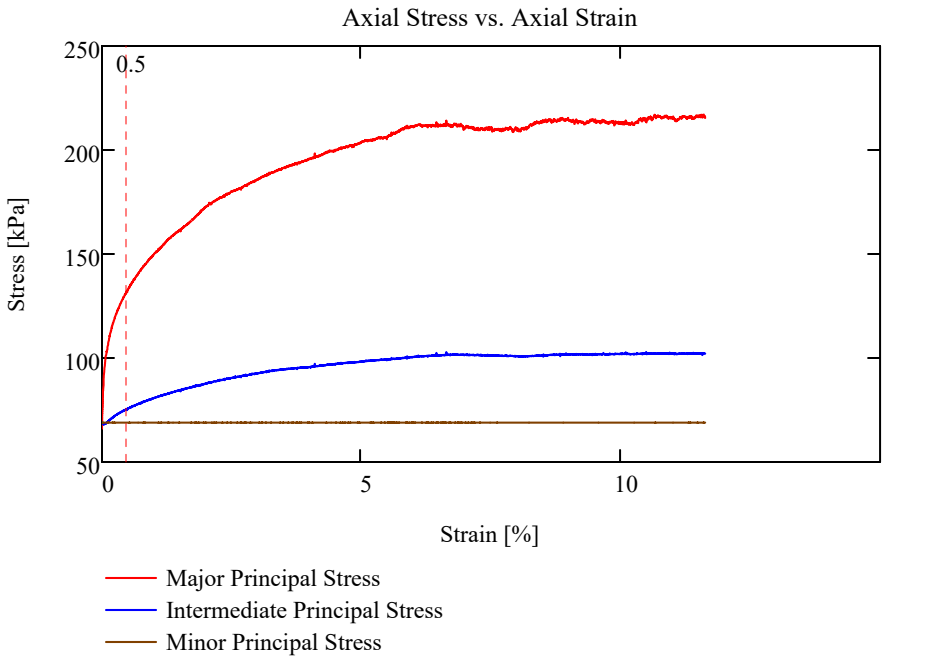
Axial Stress vs. Axial Strain
250
200
150
100
50
0.5
Stress [kPa]
0
5
10
Strain [%]
Major Principal Stress
Intermediate Principal Stress
Minor Principal Stress

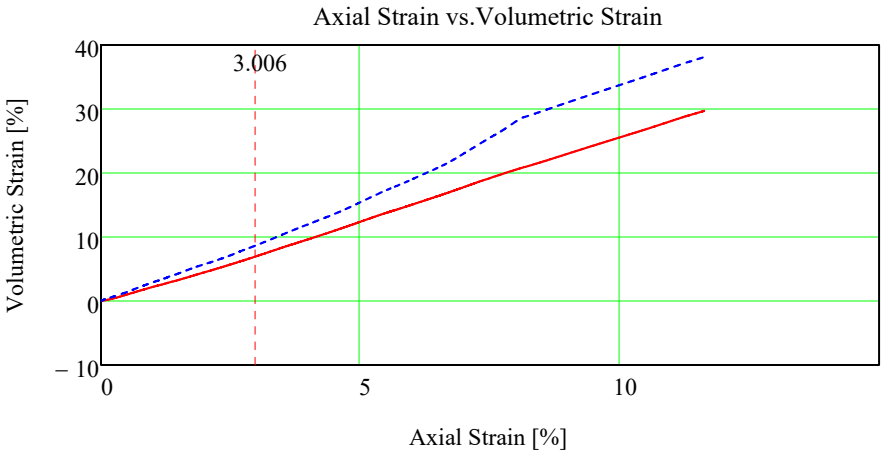
Axial Strain vs.Volumetric Strain
40
30
20
10
0
– 10
3.006
Volumetric Strain [%]
0
5
10
Axial Strain [%]

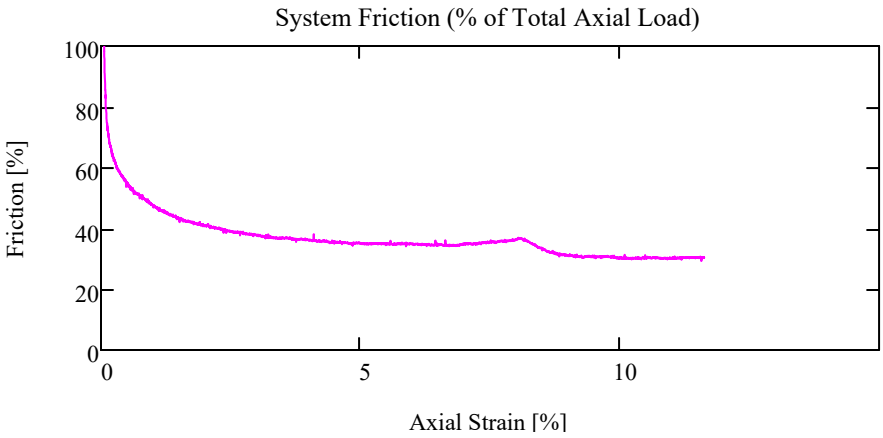

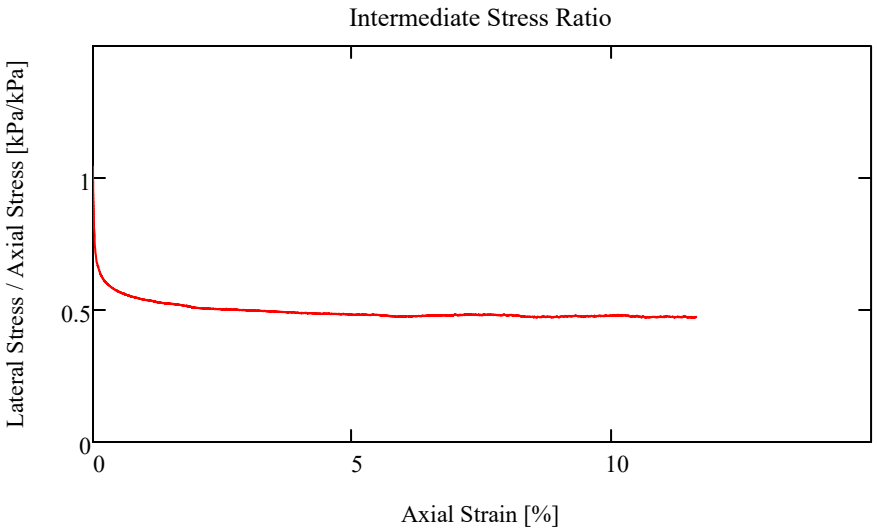

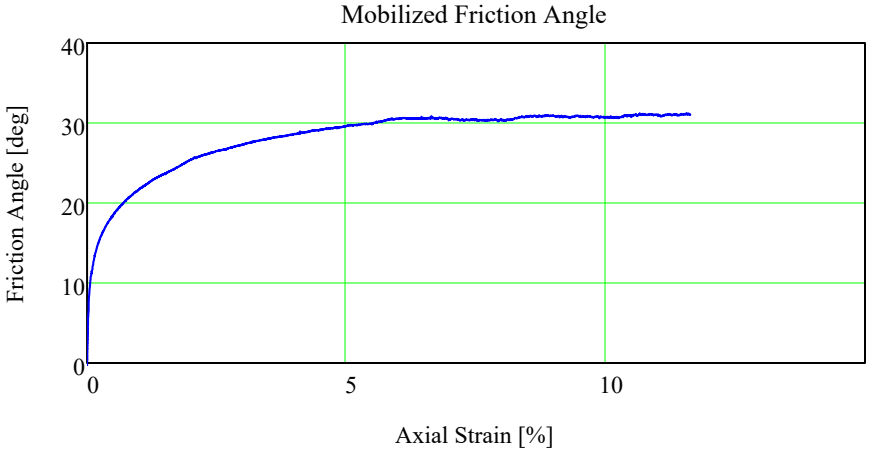

CALCULATION OF STRESS AND STRAIN AFTER THE ONSET OF LOCALIZATION

(based on Drescher, et al., 1990)

Inclination of failure plane: $\theta_e := 50deg$

Global strain at onset of shear banding: $\varepsilon_b := 0.5\%$

Shift data vectors to correspond to the onset of shear banding:

$$\text{Locate}(v,\varepsilon) := \begin{| i \leftarrow 0 \\ L \leftarrow 0 \\ \text{for } m \in 0..\text{last}(v) \\ \quad \text{if } v_m \geq \varepsilon \\ \quad\quad L \leftarrow m \\ \quad\quad \text{return } L \end{|}$$

$\text{new} := \text{Locate}(\varepsilon_1, \varepsilon_b)$

$\text{new} = 254$

$u_h := \text{disp}^{\langle 6 \rangle}$ $\quad p := \text{new}..\text{nrows} - 1$

$u_{hh_{p-new}} := u_{h_p}$ $\quad u_{aa_{p-new}} := u_{a_p}$ $\quad \sigma_{11_{p-new}} := \sigma_{1_p}$ $\quad \sigma_{33_{p-new}} := \sigma_{3_p}$

$t_{h_{p-new}} := \text{time}_p - \text{time}_{new}$ $\quad \varepsilon_{1h_{p-new}} := \varepsilon_{1_p} - \varepsilon_{1_{new}}$

Calculate incremental axial and sled displacements:

$i := 0..\text{last}(u_{hh}) - 1$ $\quad \Delta u_{h_i} := u_{hh_{i+1}} - u_{hh_i}$ $\quad \Delta u_{a_i} := u_{aa_{i+1}} - u_{aa_i}$

Normal stress on failure plane: $\sigma_n := \sigma_{11} \cdot \cos(\theta_e)^2 + \sigma_{33} \cdot \sin(\theta_e)^2$

Shear stress on failure plane: $\sigma_s := (\sigma_{11} - \sigma_{33}) \cdot \cos(\theta_e) \cdot \sin(\theta_e)$

Friction on the shear band: $\phi_s := \text{atan}\left(\frac{\overrightarrow{\sigma_s}}{\sigma_n}\right)$

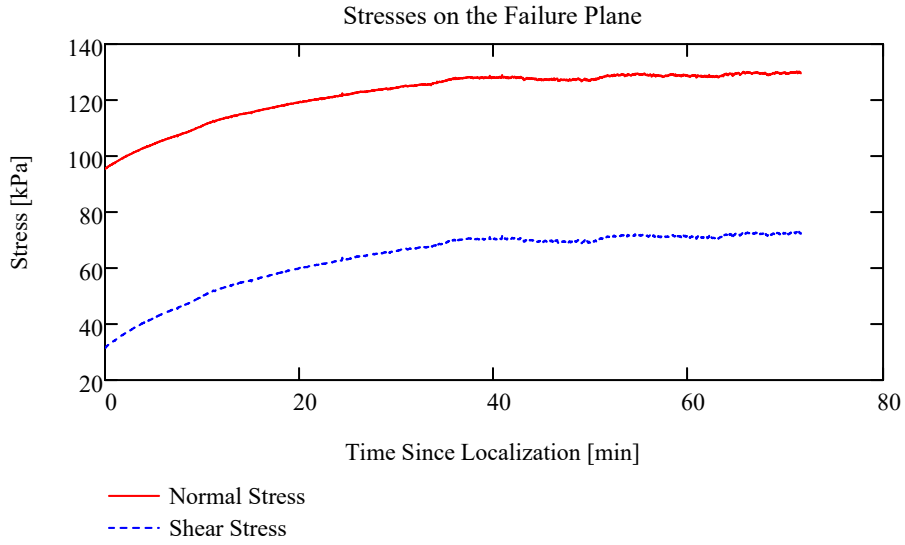
Stresses on the Failure Plane
Stress [kPa]
140
120
100
80
60
40
20
0
20
40
60
80
Time Since Localization [min]
Normal Stress
Shear Stress

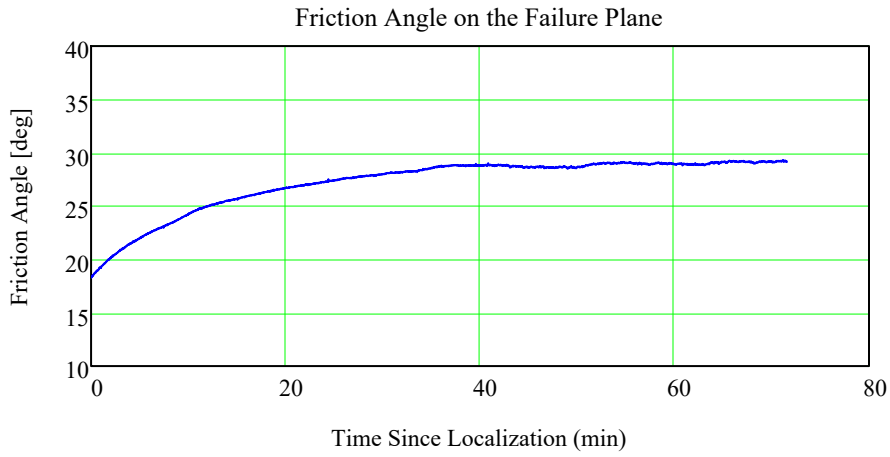
Friction Angle on the Failure Plane
Friction Angle [deg]
40
35
30
25
20
15
10
0
20
40
60
80
Time Since Localization (min)

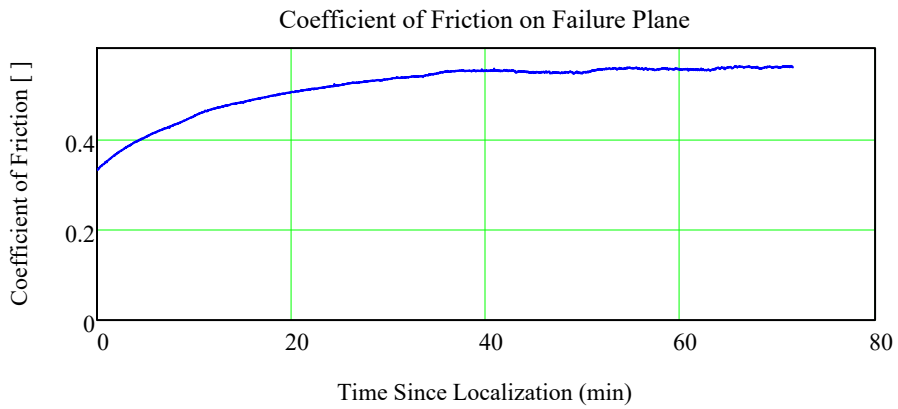
Coefficient of Friction on Failure Plane
Coefficient of Friction [ ]
0.4
0.2
0
0
20
40
60
80
Time Since Localization (min)